The Pennsylvania State University

The Graduate School

Eberly College of Science

COPOLYMERIZATION OF POLAR AND NONPOLAR VINYL MONOMERS: MECHANISITIC INSIGHT AND FREE RADICAL POLYMERIZATION

A Thesis in

Chemistry

by

Megan L. Nagel

Submitted in Partial Fulfillment
of the Requirements
for the Degree of

Doctor of of Philosophy

August 2006

The thesis of Megan Nagel has been reviewed and approved* by the following**:**

Ayusman Sen
Professor of Chemistry
Head of the Department of Chemistry
Thesis Advisor
Chair of Committee

John Badding
Associate Professor in Chemistry

Alan Benesi
Director, NMR Facility
Lecturer in Chemistry

T. C. Mike Chung
Professor of Materials Science

*Signatures are on file in the Graduate School.

ABSTRACT

[1,2-bis(4,4-dimethyl-2-oxazolin-2-yl)ethane]copper(II)dichloride, in the presence of MAO, is an effective catalyst for the homopolymerization of methyl methacrylate (MMA) and methyl acrylate (MA), and for the copolymerization of the latter with ethene and propene. The latter copolymers were acrylate rich. Several other metal salts also catalyze the homopolymerization of MMA in the presence of MAO. The addition of galvinoxyl had no effect on the polymerization ability of these systems. EPR experiments suggest that the commonly employed radical traps, galvinoxyl, DPPH, and TEMPO, are destroyed by methyl aluminoxane (MAO), thereby enabling radical polymerizations to proceed despite the addition of these traps to the reaction mixture. Thus, probing for a radical polymerization mechanism through the use of stable radical traps may not be valid for such systems employing MAO.

The addition of the Lewis acid, $Sc(OTf)_3$, to 2,2'-azobis(2-methylpropionitrile) (AIBN) initiated copolymerizations of both methyl acrylate (MA) and methyl methacrylate (MMA) with 1-alkenes results in increased reaction rate and increased incorporation of the latter monomer into the polymer backbone. As little as 4 mol% of the Lewis acid is effective in forming a nearly alternating copolymer of MA and ethene at 67% MA conversion. This procedure allows for the control of copolymer composition independent of the starting monomer feed ratio.

Several palladium-phosphine complexes were synthesized and subsequently treated with methyl 2-bromobutyrate to form a complex analogous to the product formed from the single insertion of methyl acrylate into a palladium-methyl bond. For all of the ligands used, the complexes were shown to decompose by two distinct pathways, β-hydrogen elimination and homolytic cleavage of the palladium-alkyl bond, which forms active radicals. The preferred decomposition pathway can be changed dramatically depending on the properties of the ligand employed.

One of the few late-transition metal catalysts reported to successfully insert methyl acrylate to form a stable complex is a palladium diimine system that forms a stable six-membered chelate. Upon disruption of this chelate with PPh_4Br, the complex undergoes a rearrangement by "chain-walking". The palladium-alkyl of both the opened chelate and the final rearrangement product are shown to homolytically cleave. This demonstrates the propensity of these compounds to decompose by radical methods not only when the ester group is α to the palladium, but also when it is removed from the metal center.

TABLE OF CONTENTS

LIST OF FIGURES

LIST OF TABLES

ACKNOWLEDGEMENTS

There are so many people that have made an impact on me throughout my time in graduate school. First, I would like to thank my graduate preceptor, Ayusman Sen for all of his knowledge and patience with me. I could not have imagined working for a more supportive person. My undergraduate student, Dawn Poli, was a fun change of pace to have in the lab, and she greatly contributed both to my sanity, and the discoveries in this thesis. I've enjoyed working with all of the Sen group members that I've had a chance to know. I'd specifically like to thank Dr. Jeffrey Funk, Dr. Sachin Borkar, and my "polymer pal", Rong Luo for their assistance, advice and input.

I have been fortunate enough to be part of an active collaboration with the Columbus Team from the Rohm and Haas company. They were always able to make me feel like my research was useful and important. I would especially like to thank Tom Kirk for his time in setting up the large scale reactor and teaching me how to use it and Brian Goodall for his career advice and support. The Rohm and Haas company also contributed to my funding while in graduate school along with, the National Science Foundation and the Department of Energy. I would also like to acknowledge the Braddock Graduate Fellowship, the Roberts Graduate Fellowship, and the Dalalian Research Fellowship for providing additional monetary resources.

Without the support of my endlessly encouraging husband, Micah, I don't know how I would have made it this far. I would like to thank him for always believing

in me, proofreading my papers even when he didn't know what they meant, and making me laugh no matter how frustrated I was. Also, I must give an enormous thank you to my wonderful family, especially my mother and father, Pat and Bob Majcher. I'm so glad you never took me seriously when I said I was going to quit, and were always excited about even the most meaningless news from the lab. In addition, I have been so fortunate to have many great friends support me while I was at Penn State. They include, Sheryl Rummel, Nicole Brown, Kimi Grant, and Kate Oberholtzer. You all have provided me with excellent advice, but more importantly, excellent distraction from research!

Finally I would like to thank God, the author and perfector of this universe. Without His divine order that graces even the smallest molecule, none of my research could have been possible.

CHAPTER 1 – INTRODUCTION

All of the chapters in this thesis deal with different projects that I have worked on throughout my time in graduate school at Penn State University. The common theme for all of the research I have done is the study of the copolymerization of polar and non-polar olefins. I have specifically focused on methyl acrylate (MA), methyl methacrylate (MMA), ethylene and α-olefin monomers. In the course of my research, it became clear that what I was working on was actually a cautionary tale of how to approach the subject of metal-catalyzed insertion polymerization of acrylates and nonpolar vinyl monomers. This is especially evident in chapters 2, 4, and 5. On a slightly different note, chapter 3 is a study of the free-radical copolymerization of acrylates and α-olefins in the presence of the Lewis acid, scandium(III)triflate ($Sc(OTf)_3$).

Chapter 2 starts as a study of a novel, copper-based catalyst we synthesized in our lab. The design of the catalyst was based on a system developed at Exxon-Mobil which showed promise for the copolymerization of acrylates and α-olefins.[1] For both ours and the Exxon-Mobil system, methylaluminoxane (MAO) was used as a cocatalyst. We examine both the homopolymerization of MMA and the copolymerization of MA and MMA with nonpolar olefins under various reaction conditions. ^{1}H NMR was used to determine the amount of each monomer along the polymer backbone, and gel permeation chromatography (GPC) was used to determine polymer molecular weights and molecular weight distributions.

As it turns out, the polymers we were producing with this copper catalyst were most likely radically initiated, and this project ended as a very interesting study of the effect (or lack thereof) of radical traps when used in the presence of the cocatalyst, MAO. This involved the use of EPR spectroscopy to identify when and if radicals were present in the polymerization system.

In 2001, our lab published a paper introducing the free-radical copolymerization of acrylates and α-olefins under relatively mild conditions.[2] Although this type of copolymerization was shown to be possible, the amount of each monomer incorporated into the polymer backbone was not able to be controlled. Chapter 3 of this thesis introduces a similar free-radical system, but the Lewis acid, $Sc(OTf)_3$ has been added to the polymerization system in catalytic amounts. $Sc(OTf)_3$ has been previously reported to increase the amount of isotacticity for the homopolymerization of methyl methacrylate.[3] This Lewis acid is soluble in acrylate solutions because of its ability to coordinate to the ester functionality of the acrylate monomer. We studied the copolymerization of MA and MMA with α-olefins with various loadings of $Sc(OTf)_3$. Conventional controlled radical polymerization techniques were also employed with this method. Depending on the amount of the Lewis acid present, the amount of each monomer in the copolymer can be controlled. Also, the presence of the $Sc(OTf)_3$ has a dramatic effect on the copolymer yield.

A detailed study of palladium-alkyl bond stability is discussed in chapters 4 and 5. The work done for chapter 4 includes the study of a very general palladium system containing commercially available phosphine ligands with varying electronic and steric properties. We were able to simulate the insertion of methyl acrylate into a palladium

alkyl bond by oxidatively adding the alkyl bromide, methyl 2-bromobutyrate, to the palladium-phosphine complex. We were then able to study the instability and decompositions products of the system.

In all of the cases that we studied, the palladium-alkyl bond decomposed by either β-hydrogen elimination or homolytic cleavage, giving active radicals. Using ^{31}P NMR and ^{1}H NMR we were able to follow the formation of the complex, and the decomposition products were identified by gas chromatography. We found that the pathway of decomposition is rather dependent not only on the properties of the ligand, but also the amount of ligand present.

The final chapter is also a study of the instability of palladium-alkyl complexes, but in this case we were interested in studying a more specific system. There exists a palladium system with a bulky diimine ligand that is known to insert MA and subsequently copolymerize acrylates and nonpolar olefins.[4] Unlike the host of other late-transition metal systems reported, the palladium-alkyl bond in this system does not suffer from decomposition because of a stable six-membered chelate that is formed following MA insertion. The project described in chapter 5 involves the disruption of this chelate and examines the decomposition that follows. Both 1-D and 2-D ^{1}H NMR provided invaluable information about the steps involved in the decomposition mechanism and also kinetic and thermodynamic details.

The chapters in this thesis represent and outline of the polymerization research in the Sen research group. The work with $Sc(OTf)_3$ shows the effectiveness of free-radical chemistry for the copolymerization of acrylates with nonpolar olefins by pushing it to its limits. Illustrating the short-comings of radical traps, as described in chapter 2, provides

useful insight for continued work in exploring reaction mechanisms where MAO is used as a cocatalyst. Finally, gaining greater understanding of the Pd-alkyl bond that has an ester group α to the metal center will hopefully provide insight for future ligand design of catalyst systems for insertion polymerization of acrylates and copolymerization with α-olefins.

REFERENCES

1. Stibrany, R. T.; Schulz, D. N.; Kacker, S.; Patil, A. O.; Baugh, L. S.; Rucker, S. P.; Zushma, S.; Berluche, E.; Sissano, J. A. *Macromolecules* **2003**, *36*, 8584-8586.
2. Liu, S. H.; Elyashiv, S.; Sen, A. *J. Am. Chem. Soc.* **2001**, *123*, 12738.
3. Isobe, Y.; Nakano, T.; Okamoto, Y. *J. Polym. Sci., Part A: Polym. Chem.* **2001**, *39*,1463.
4. Mecking, S.; Johnson, L. K.; Wang, L.; Brookhart, M. *J. Am. Chem. Soc.* **1998**, *120*, 888-899.

CHAPTER 2 – METAL-MEDIATED POLYMERIZATION OF ACRYLATES: RELEVANCE OF RADICAL TRAPS

2.1 – INTRODUCTION

Metal-mediated vinyl insertion polymerization of polar monomers, especially acrylates, is an area of great current interest because of the control over polymer microstructure, molecular weight, and polydispersity that such systems are expected to provide.[1] Recently, several reports have appeared claiming insertion polymerization of acrylates by late transition metal-based systems.[2,3,4] The primary evidence cited against an alternative radical mechanism has been the failure of radical traps to halt the polymerization. While the reliability of phenolic radical traps, such as di-tert-butyl phenol has been questioned,[5] stable radicals such as galvinoxyl, DPPH, and TEMPO (TABLE 2.1) have been used as benchmark traps for probing the intermediacy of radicals in polymerizations. The test is based on the hypotheses that the radical trap reacts only with radical species in the medium and is not affected by other species. However, as illustrated below for a copper-based system, this may not hold for systems where the possibility of deactivation of the trap, for example by reduction to the anion, exists. Our work calls into question the widespread use of radical traps for probing reaction mechanism in metal-based systems employing methyl aluminoxane (MAO).

TABLE 2.1 – Chemical Structure of Common Radical Traps

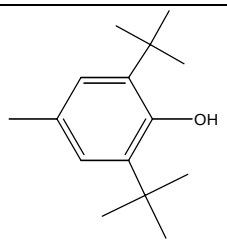   2,6-di-tert-butyl phenol
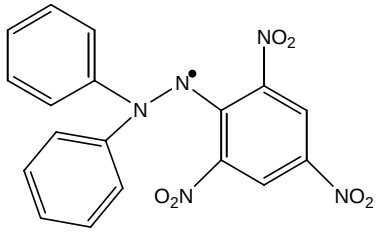   2,2, diphenyl-1-picrylhydrazyl (DPPH)
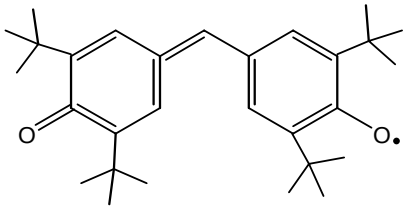   galvinoxyl
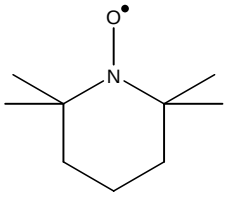   2,2,6,6-Tetramethylpiperidine 1-oxyl (TEMPO)

2.2 – RESULTS AND DISCUSSION

2.2.1 – HOMOPOLYMERIZATION OF METHYL ACRYLATE AND METHYL METHACRYLATE

The compound, $Cu(DMOX)Cl_2$, is an air stable, distorted tetrahedral complex, whose crystal structure is shown in FIGURE 2.1. Crystallographic data is presented in TABLE 2.5 to 2.9. At a relatively low MAO to copper ratio of 20, an active system for the homopolymerization of methyl methacrylate (MMA) is formed from this species. Polymerizations were carried out at various temperatures from ambient to 80º C with good monomer conversions (TABLE 2.2). A comparison with the polymers obtained using either the radical initiator AIBN or a combination of AIBN and MAO showed that the polymers formed by the copper-based system were slightly more syndiotactic (e.g., rr dyad was 5-8% higher) for all three temperatures examined (60, 70, and 80°C) (see TABLE 2.2). We also observed that the addition of MAO to the copper catalyst is vital for any polymerization activity.

The system is also effective for the homopolymerization of methyl acrylate (MA) and its copolymerization with ethene and propene (TABLE 2.3). However, the poly(methyl acrylate) obtained is atactic. The introduction of ethene or propene into the MA homopolymerization system resulted in the formation of acrylate-rich copolymers in greatly reduced yields. Additionally, the level of olefin incorporation in the copolymers was similar to that observed by us and others for well-documented radical polymerization systems.[6,7,8]

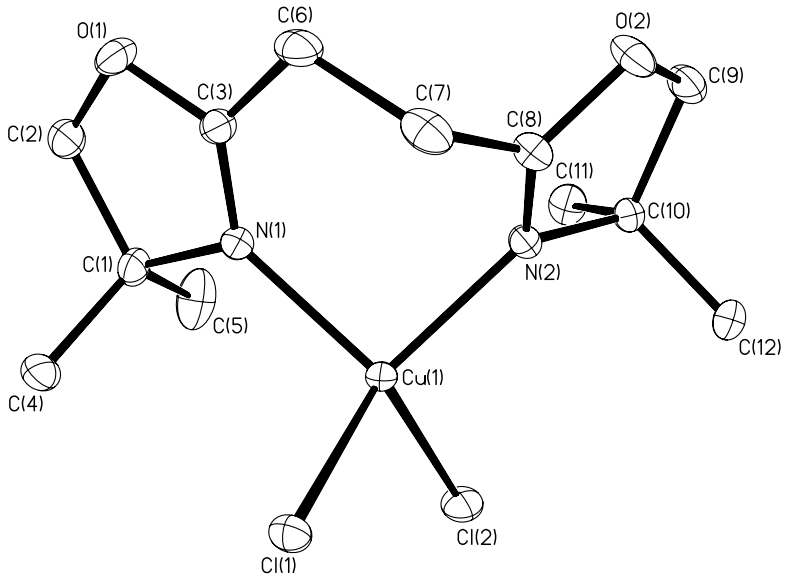

FIGURE 2.1 – ORTEP diagram for the X-ray crystallography structure determination of sen18a, [1,2-bis(4,4-dimethyl-2-oxazolin-2-yl)ethane]copper(II)dichloride**.**

TABLE 2.2 – Homopolymerization of Methyl Methacrylate

Entry	Initiator/ Catalyst	Cocat[b]	Inhibitor[c]	Temp (ºC)	Yield (%)	M_w[d] x 10^{-3}	M_w/M_n[d]	Tacticity[e] %mm	%mr	%rr
1	$Cu(DMOX)Cl_2$	MAO		50	55	316	4.3	5.3	26.6	68.1
2	$Cu(DMOX)Cl_2$	MAO		60	60	278	3.8	4.6	29.9	65.5
3	$Cu(DMOX)Cl_2$	MAO		70	48	389	4.4	5.3	30.6	64.1
4	$Cu(DMOX)Cl_2$	MAO		80	42	257	3.7	5.9	31.6	62.5
5	$Cu(DMOX)Cl_2$			40	N.R.					
6	$Cu(DMOX)Cl_2$	MAO	Galvinoxyl	40	41	131	4.2	5.4	30.6	63.9
7	AIBN		Galvinoxyl	60	N.R.					
8	AIBN			60	77	73	1.9	5.3	34.4	60.4
9	AIBN			70	77	62	1.5	7.0	34.5	58.2
10	AIBN			80	81	32	1.5	6.3	36.4	57.3
11	AIBN	MAO		60	72	114	1.3	4.9	33.9	61.2
12	$Cu(OAc)_2$	MAO		60	25	170	3.9	5.9	37.9	56.2

[a] Reaction Conditions: 0.030mmol of AIBN or 0.022 mmol of Cu compound ; PhCl, 5 mL; 0.01 mol of MMA; 21 h in drybox. [b]80mg of 30% MAO solution (0.42 mmol). [c]1 equivalent galvinoxyl. [d]Determined by GPC against polystyrene standards using refractive index detector. [e]Calculated from ^{1}H NMR integration of α-methyl peaks.

TABLE 2.3 – Homo- and copolymerization of methylacryate using Cu(DMOX)Cl_2.

Comonomer	Temp (ºC)	MA Conv. (%)	Alkene Incorp. (mol)%	M_w (x 10^{-3}) (M_w/M_n)[c]	Tacticity[d] threo	racemic	erythro
	50	50		126 (1.7)	25.2%	48.6%	26.2%
	60	49		122 (1.8)	25.8%	48.3%	25.7%
	70	47		105 (3.2)	25.5%	49.6%	24.9%
Ethene (500 psi / 0.163 M)	40	20	16.4	126 (2.1)			
Propene (2 g /0.037 M)	60	27	22.5	257 (3.7)			

[a] Reaction Conditions: Cu(DMOX)Cl_2, 0.022 mmol; 30% MAO solution, 0.42 mmol (80mg); PhCl, 5 mL; 0.01 mol of MA; 21 h in drybox. [b]Calculated from integration of ^{1}H NMR resonances. [c]Determined by GPC against polystyrene standards using refractive index detector. [d]Calculated from ^{1}H NMR integration of α-methyl peaks.[10]

2.2.2 – STUDY OF THE POLYMERIZATION SYSTEM BY EPR

The addition of MAO to the EPR active $Cu(DMOX)Cl_2$ resulted in the formation of an EPR silent Cu(I) species (FIGURE 2.2). This occurred on the same time scale as the onset of polymerization suggesting that the reduction of Cu(II) to Cu(I) alkyl is necessary for polymerization. No further change in EPR spectrum occurred in the course of the polymerization; however, the Cu(I) species was reoxidized to Cu(II) upon exposure of the polymerization system to air as shown in FIGURE 2.3.

In order to examine whether free radicals were involved in the polymerization process, 1 equivalent of galvinoxyl per Cu was added to the reaction mixture. As shown in TABLE 2.1, a similar yield of PMMA was obtained. In contrast, an equivalent amount of galvinoxyl totally quenched the polymerization activity of AIBN. The above results with galvinoxyl pose a dilemma. The polymerization profile, specifically the failure to homopolymerize unactivated olefins (e.g., ethene or 1-alkenes) or to incorporate them in significant amounts in copolymerizations, clearly suggested a radical mechanism. In contrast, the strongest (and the most widely accepted) evidence against a radical mechanism was the failure to stop or slow the MMA homopolymerization by adding galvinoxyl. However, we observed the disappearance, at ambient temperature, of the EPR signal of galvinoxyl (0.021 mmol) when a solution of it in chlorobenzene was added to a solution prepared by dissolving $Cu(DMOX)Cl_2$ (0.022 mmol) and MMA (0.01 mol) in 5 mL of chlorobenzene followed by the addition of 80 mg of a 30% MAO solution. In order to probe the generality of the deactivation of galvinoxyl by the combination of a metal species and MAO, $Cu(OAc)_2$, $Ni(acac)_2$, $Co(acac)_2$, and $Fe(OAc)_2$ were also

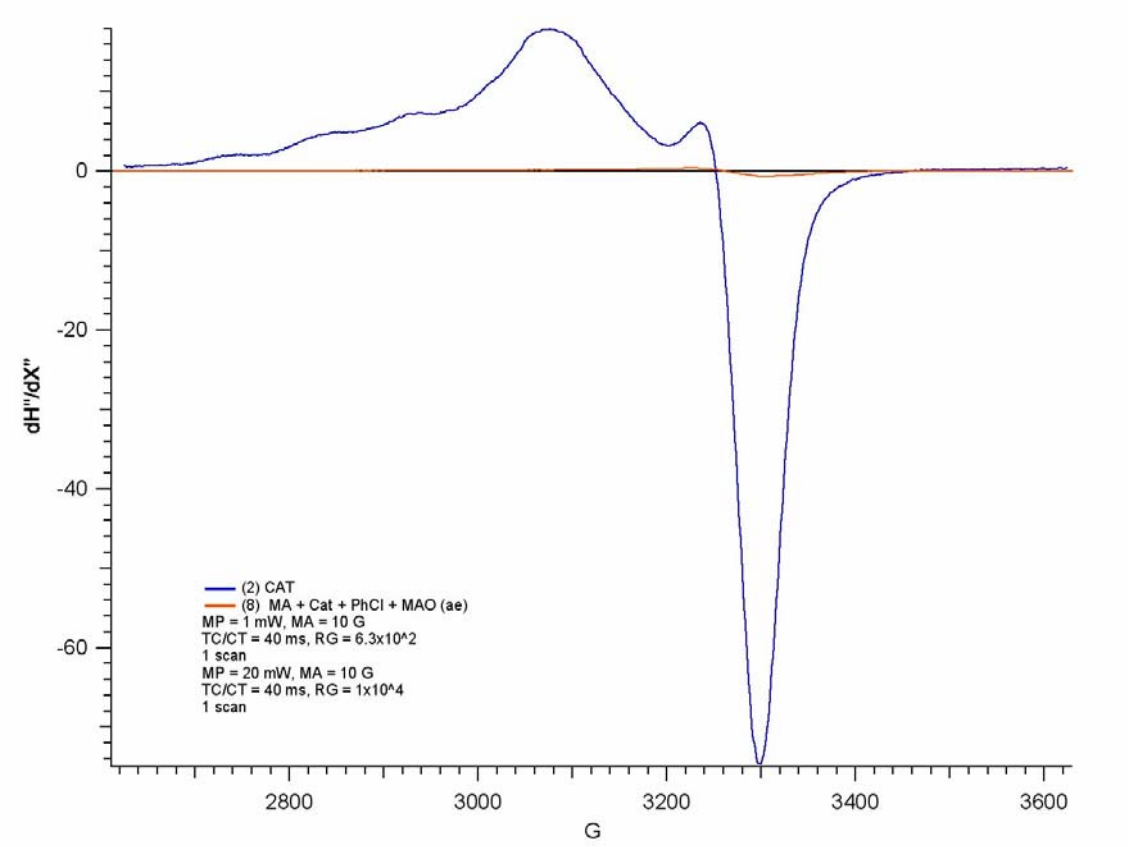

FIGURE 2.2 – EPR spectrum forCu(DMOX)Cl_2 in PhCl (blue) and the disappearance of signal following the additon of MAO to the system (orange).

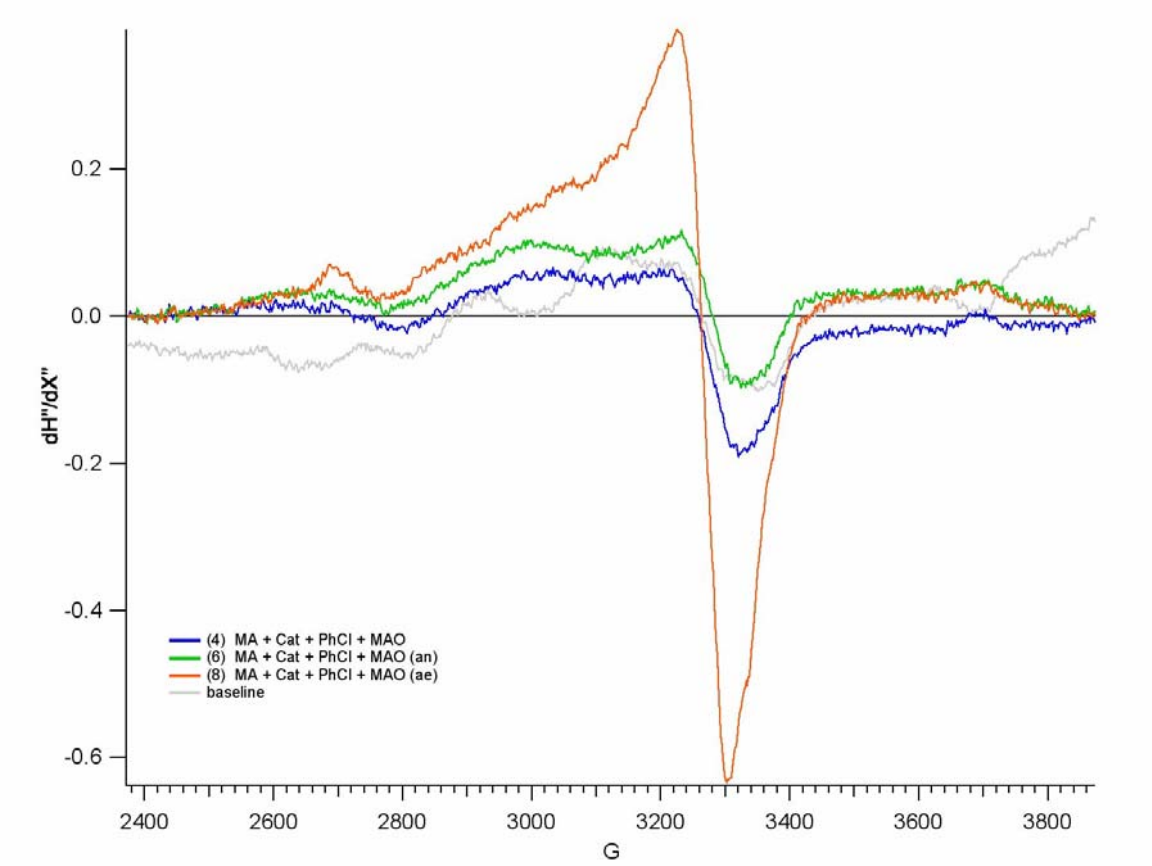

FIGURE 2.3 – EPR spectra for a) Baseline (gray) b)Cu(DMOX)Cl_2 following the addition of MAO in PhCl (blue) c) after 4 hours anaerobically (green), and d) after exposure to air for several minutes(orange).

employed under similar reaction conditions. In every case the EPR signal of galvinoxyl disappeared and polymer formation was observed.

The above experiments led us to suspect that MAO was responsible for the deactivation of galvinoxyl through reduction. Indeed, EPR experiments demonstrated that the radical signal of galvinoxyl, as well as two other commonly employed radical traps, DPPH and TEMPO disappeared upon the addition of excess MAO. Additionally, we observed that AIBN-initiated homopolymerization of MMA was completely halted when any one of the above radical traps was added *but polymer was obtained when MAO was also present in the reaction mixture* (conditions: 10 mmol MMA, 0.024 mmol AIBN, 0.021-0.026 mmol galvinoxyl, DPPH, or TEMPO, 5 mL PhCl, 18 h, 60°C, 80 mg of 30% MAO in PhCl) (TABLE 2.4).

Finally, in order to ascertain the fate of galvinoxyl in its reaction with MAO, 0.021 mmol of galvinoxyl was mixed with 80 mg of 30% MAO in PhCl. After stirring for 10 min at ambient temperature, the mixture was added to an excess of 0.1 M aqueous HCl, and the organic product was isolated. Its mass spectal analysis indicated it to be the phenol derived from galvinoxyl (m/z = 423 (MH^+)), suggesting its reduction to the anion by MAO, which is a strong reducing agent (FIGURE 2.4).

TABLE 2.4 - Usefulness of Radical Traps in the Presence of MAO

Entry	Radical Trap	MAO[b]	Polymer
a	DPPH (0.023mmol)	NO	NO
b	DPPH (0.025mmol)	YES	YES
c	TEMPO (0.026mmol)	NO	NO
d	TEMPO (0.026mmol)	YES	YES
e	GALVINOXYL (0.021mmol)	NO	NO
f	GALVINOXYL (0.021mmol)	YES	YES

[a]0.024mmol AIBN in 5mL PhCl, 10mmol MMA stirred for 18 hours at 60°C [b]80mg of 30% MAO solution in PhCl

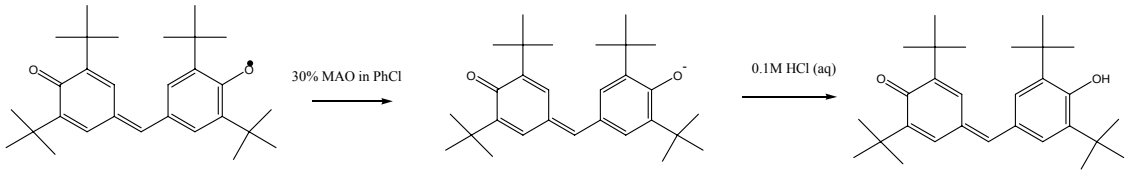

FIGURE 2.4 – Reduction of galvinoxyl with MAO and subsequent treatment with a strong acid to give the phenol.

2.3 - CONCLUSIONS

The use of radical traps such as galvinoxyl, DPPH, and TEMPO as a probe for radical mechanism in metal-based systems employing MAO can lead to the wrong conclusion. We had earlier reported that radical traps can react with metal-hydrides and halt or slow down metal-centered nonradical reactions.[11] Now, we show that radical traps may fail to intercept even radical reactions that proceed in the presence of MAO. Clearly, it is necessary to rely on several independent lines of evidence before coming to a firm mechanistic conclusion. For example, the formation of copolymers whose compositions vary significantly from that predicted from the radical reactivity ratios must be demonstrated before a non-radical mechanism can be invoked.

2.4 – EXPERIMENTAL PROCEDURES

2.4.1 – SYNTHESIS OF COPPER CATALYST

In a round bottom flask $CuCl_2 \bullet 2H_2O$ (3.7 mmol) was dissolved in 35 mL of anhydrous ethanol at room temperature. This was followed by the addition of 4 mL of triethylorthoformate. To this solution, 1,2-bis(4,4-dimethyl-2-oxazolin-2-yl)ethane (DMOX) (1.2 mmol) (Aldrich, used as received) was then added. A bright yellow precipitate formed almost immediately. The precipitate was collected by vacuum filtration, washed with pentane and dried under high vacuum. Yield: 50%. C, H, N, Cl analyses were satisfactory.

2.4.2 – POLYMER SYNTHESIS AND CHARACTERIZATION

Polymerizations were performed using oven-dried glassware in a drybox. For those carried out with the copper compound, a vial was charged with a stirbar and $Cu(DMOX)Cl_2$ (0.022 mmol) followed by the addition of 5 mL of distilled chlorobenzene to form a yellow solution. Subsequently, MMA (0.01 mol) was added to this solution. A 30% MAO solution was prepared separately by the addition of 300 mg of dry MAO to 970 mg of chlorobenzene. To the $Cu(DMOX)Cl_2$/MMA solution, 80 mg of the MAO solution was added thus inducing a quick color change from yellow to green to colorless. The reaction was then sealed and allowed to react at the appropriate temperature for 21 h. The formed polymer was precipitated in a large excess of 5% HCl in methanol and stirred

overnight to dissolve any catalyst residues. The insoluble polymer was filtered and dried under vacuum overnight. For those reactions initiated with other metal species or AIBN, similar procedures were followed.

NMR spectra of polymers were recorded on a Bruker DPX 300 MHz spectrometer to determine the tacticity from triad distributions. Polymer molecular weights were determined against a polystyrene standard by gel permeation chromatography on either a Waters Associates 600 using Millenium 32 software or Shimadzu chomatograph using EZSTART 7.2 software. Each of these instruments contained three Waters styragel HR columns at 35° C in chloroform (1 mL/minute).

2.4.3 EPR EXPERIMENTS

EPR spectra were measured with a Bruker ECS 106 with a modulation amplitude and modulation frequency of 60 gauss and 100 kHz, respectively. The spectra were measured at 77K. Four samples were prepared. The first three were prepared in a nitrogen-filled glovebox and contained, respectively, chlorobenzene (1), chlorobenzene, MMA and Cu(DMOX)Cl_2 (2), chlorobenzene, MMA, Cu(DMOX)Cl_2 and MAO (3), and finally (3) was exposed to air causing reoxidation of the copper (4). Signals were only observed for samples (2) and (4) indicating the presence of copper(II). The absence of signal for sample (3) indicated that all of the copper had been reduced to the EPR silent Cu(I).

To test for the presence of a galvinoxyl signal, a 4.3 mM solution of galvinoxyl was prepared in chlorobenzene giving a very deep purple color. The EPR of this solution

gave a single, strong signal for this organic radical. A second solution was prepared by the addition of 0.022 mmol of Cu(DMOX)Cl_2 to 5 mL of chlorobenzene followed by the addition of 0.01 mmol of MMA. 80 mg of a 30% MAO solution were then added to this solution turning the color from yellow to colorless. There was no EPR signal for this solution. The solution was briefly allowed to stir before the addition of 0.021 mmol of galvinoxyl, which resulted in a solution that was once again 4.3 mM in galvinoxyl, and bright red color. This sample was capped, quickly removed from the glovebox and placed in liquid nitrogen. An EPR spectrum of this second sample showed no signal, indicating the presence of EPR silent Cu(I), as was observed previously, and also the complete disappearance of the galvinoxyl radical. EPR experiments with other metal compounds were carried out analogously.

For reactions of radical traps with MAO only, 0.02 mmol of galvinoxyl, DPPH, and TEMPO were separately dissolved in chlorobenzene. EPR spectrum showed an organic radical peak in each case. 80 mg of 30% MAO solution was then added to each solution. These solutions were then allowed to stir for several minutes and once again EPR spectra were taken. In all cases, the EPR spectrum showed complete diappearance of the original signal.

TABLE 2.5 – Crystal Data and Structure Refinement for $Cu(DMOX)Cl_2$

Identification code	sen18a	
Empirical formula	C12 H20 Cl2 Cu N2 O2	
Formula weight	358.74	
Temperature	150(2) K	
Wavelength	0.71073 Å	
Crystal system	Monoclinic	
Space group	P2(1)/c	
Unit cell dimensions	a = 14.0146(7) Å	□= 90°.
	b = 9.5327(5) Å	□= 105.9800(10)°.
	c = 11.9678(6) Å	□ = 90°.
Volume	1537.08(14) $Å^3$	
Z	4	
Density (calculated)	1.550 Mg/m^3	
Absorption coefficient	1.767 mm^{-1}	
F(000)	740	
Crystal size	0.25 x 0.20 x 0.10 mm^3	
Theta range for data collection	1.51 to 28.28°.	
Index ranges	-18<=h<=17, -12<=k<=11, -11<=l<=15	
Reflections collected	9377	
Independent reflections	3553 [R(int) = 0.0178]	

TABLE 2.5., continued.

Completeness to theta = 28.28°	93.0 %
Absorption correction	None
Refinement method	Full-matrix least-squares on F^2
Data / restraints / parameters	3553 / 0 / 172
Goodness-of-fit on F^2	0.409
Final R indices [I>2sigma(I)]	R1 = 0.0277, wR2 = 0.0767
R indices (all data)	R1 = 0.0319, wR2 = 0.0916
Largest diff. peak and hole	0.425 and -0.218 e.$Å^{-3}$

TABLE 2.6 Atomic coordinates (x 10^4) and equivalent isotropic displacement parameters ($Å^2$x 10^3) for $Cu(DMOC)Cl_2$.

	x	y	z	U(eq)
Cu(1)	2260(1)	463(1)	6326(1)	19(1)
Cl(1)	884(1)	-274(1)	6720(1)	27(1)
Cl(2)	3390(1)	-353(1)	7887(1)	32(1)
N(1)	1893(1)	80(2)	4624(1)	23(1)
N(2)	2839(1)	2340(2)	6173(1)	21(1)
O(1)	1525(1)	274(2)	2688(1)	39(1)
O(2)	2685(1)	4505(2)	5425(2)	32(1)
C(1)	2090(2)	-1365(2)	4228(2)	28(1)
C(2)	1934(2)	-1137(3)	2920(2)	43(1)
C(3)	1570(2)	858(3)	3728(2)	28(1)
C(4)	1335(2)	-2395(2)	4452(2)	32(1)
C(5)	3145(2)	-1799(3)	4848(3)	48(1)
C(6)	1232(2)	2339(3)	3660(2)	34(1)
C(7)	1241(2)	3024(2)	4819(2)	32(1)

TABLE 2.6., continued.

C(8)	2282(2)	3259(2)	5532(2)	25(1)
C(9)	3741(2)	4373(2)	5992(2)	33(1)
C(10)	3851(2)	2964(2)	6655(2)	23(1)
C(11)	4618(2)	2005(3)	6365(2)	32(1)
C(12)	4059(2)	3187(3)	7962(2)	32(1)

TABLE 2.7. Bond lengths [Å] and angles [°] for $Cu(DMOX)Cl_2$.

Cu(1)-N(1)	1.9914(17)
Cu(1)-N(2)	1.9940(16)
Cu(1)-Cl(1)	2.2221(5)
Cu(1)-Cl(2)	2.2306(6)
N(1)-C(3)	1.280(3)
N(1)-C(1)	1.508(3)
N(2)-C(8)	1.279(3)
N(2)-C(10)	1.498(2)
O(1)-C(3)	1.349(3)
O(1)-C(2)	1.458(4)
O(2)-C(8)	1.336(2)
O(2)-C(9)	1.453(3)
C(1)-C(4)	1.520(3)
C(1)-C(5)	1.519(3)
C(1)-C(2)	1.535(3)
C(3)-C(6)	1.485(3)
C(6)-C(7)	1.530(4)
C(7)-C(8)	1.491(3)
C(9)-C(10)	1.546(3)
C(10)-C(11)	1.522(3)
C(10)-C(12)	1.525(3)

TABLE 2.7., continued.

N(1)-Cu(1)-N(2)	93.91(7)
N(1)-Cu(1)-Cl(1)	99.42(5)
N(2)-Cu(1)-Cl(1)	134.57(5)
N(1)-Cu(1)-Cl(2)	135.82(6)
N(2)-Cu(1)-Cl(2)	100.18(5)
Cl(1)-Cu(1)-Cl(2)	99.75(2)
C(3)-N(1)-C(1)	108.56(18)
C(3)-N(1)-Cu(1)	133.11(16)
C(1)-N(1)-Cu(1)	118.10(13)
C(8)-N(2)-C(10)	108.38(16)
C(8)-N(2)-Cu(1)	118.25(14)
C(10)-N(2)-Cu(1)	133.36(13)
C(3)-O(1)-C(2)	106.81(18)
C(8)-O(2)-C(9)	106.35(16)
N(1)-C(1)-C(4)	109.76(17)
N(1)-C(1)-C(5)	109.46(18)
C(4)-C(1)-C(5)	111.7(2)
N(1)-C(1)-C(2)	101.82(18)
C(4)-C(1)-C(2)	111.16(18)
C(5)-C(1)-C(2)	112.5(2)
O(1)-C(2)-C(1)	105.24(19)

TABLE 2.7., continued.

N(1)-C(3)-O(1)	116.7(2)
N(1)-C(3)-C(6)	129.1(2)
O(1)-C(3)-C(6)	114.18(19)
C(3)-C(6)-C(7)	115.68(18)
C(8)-C(7)-C(6)	110.22(18)
N(2)-C(8)-O(2)	117.50(19)
N(2)-C(8)-C(7)	125.44(19)
O(2)-C(8)-C(7)	116.89(18)
O(2)-C(9)-C(10)	105.03(17)
N(2)-C(10)-C(11)	109.07(16)
N(2)-C(10)-C(12)	110.09(17)
C(11)-C(10)-C(12)	111.71(18)
N(2)-C(10)-C(9)	101.40(16)
C(11)-C(10)-C(9)	112.41(19)
C(12)-C(10)-C(9)	111.67(18)

Symmetry transformations used to generate equivalent atoms:

TABLE 2.8. Anisotropic displacement parameters ($Å^2 x\ 10^3$) for $Cu(DMOX)Cl_2$.

	U^{11}	U^{22}	U^{33}	U^{23}	U^{13}	U^{12}
Cu(1)	23(1)	17(1)	17(1)	1(1)	5(1)	-1(1)
Cl(1)	28(1)	28(1)	29(1)	1(1)	12(1)	-4(1)
Cl(2)	35(1)	32(1)	26(1)	10(1)	0(1)	1(1)
N(1)	24(1)	24(1)	20(1)	0(1)	6(1)	-5(1)
N(2)	22(1)	19(1)	22(1)	1(1)	5(1)	-2(1)
O(1)	44(1)	53(1)	18(1)	2(1)	6(1)	-15(1)
O(2)	33(1)	19(1)	43(1)	8(1)	7(1)	-2(1)
C(1)	32(1)	29(1)	23(1)	-8(1)	10(1)	-5(1)
C(2)	69(2)	39(1)	27(1)	-11(1)	22(1)	-22(1)
C(3)	25(1)	35(1)	21(1)	2(1)	4(1)	-11(1)
C(4)	45(1)	23(1)	31(1)	-2(1)	15(1)	-5(1)
C(5)	33(1)	54(2)	56(2)	-27(1)	10(1)	9(1)
C(6)	29(1)	36(1)	31(1)	14(1)	-3(1)	-7(1)
C(7)	22(1)	26(1)	44(1)	11(1)	5(1)	4(1)
C(8)	26(1)	20(1)	29(1)	2(1)	8(1)	-1(1)
C(9)	34(1)	26(1)	34(1)	4(1)	2(1)	-9(1)
C(10)	24(1)	23(1)	22(1)	-1(1)	5(1)	-6(1)

TABLE 2.8., continued.

C(11)	26(1)	37(1)	35(1)	-4(1)	10(1)	-1(1)
C(12)	39(1)	31(1)	24(1)	-6(1)	6(1)	-7(1)

TABLE 2.9. Hydrogen coordinates (x 10^4) and isotropic displacement parameters ($Å^2$x 10^3) for $Cu(DMOC)Cl_2$.

H(2A)	2572	-1211	2719	52
H(2B)	1467	-1840	2464	52
H(4A)	1449	-2516	5291	48
H(4B)	1407	-3301	4097	48
H(4C)	664	-2031	4112	48
H(5A)	3208	-1929	5678	72
H(5B)	3607	-1067	4750	72
H(5C)	3303	-2681	4518	72
H(6A)	547	2384	3142	41
H(6B)	1659	2901	3294	41
H(7A)	885	3931	4674	38
H(7B)	894	2410	5248	38
H(9A)	3977	5161	6536	39
H(9B)	4125	4361	5411	39
H(11A)	4660	1128	6803	48
H(11B)	5266	2470	6576	48
H(11C)	4420	1800	5530	48

TABLE 2.9. continued.

H(12A)	4122	2275	8354	47
H(12B)	3510	3713	8122	47
H(12C)	4677	3716	8250	47

2.5 – REFERENCES

1. (a) Boffa, L. S.; Novak, B. M. *Chem. Rev*. **2000**, *100*, 1479. (b) Ittel, S. D.; Johnson, L. K.; Brookhart, M. *Chem. Rev*. **2000**, *100*, 1169.

2. Stibrany, R. T.; Schulz, D. N.; Kacker, S.; Patil, A. O.; Baugh, L. S.; Rucker, S. P.; Zushma, S.; Berluche, E.; Sissano, J. A. *Macromolecules* **2003**, *36*, 8584-8586.

3. Kim, I.; Hwang, J. M.; Lee, J. K.; Ha, C. S.; Woo, S. I. *Macromol Rapid Comm* **2003**, *24*, 508-511.

4. (a) Carlini, C.; Martinelli, M.; Galletti A. M. R.; Sbrana, G. *J. Polym. Sci. A., Polym. Chem.* **2003**, *41*, 2117-2124. (b) Carlini, C.; Martinelli, M.; Galletti A. M. R.; Sbrana, G. *J. Polym. Sci. A., Polym. Chem.* **2003**, *41*, 1716-1724.

5. Matyjaszewski, K. *Macromolecules* **1998**, 31, 4710-4717.

6. Liu, S.; Elyashiv, S.; Sen, A. *J. Am. Chem. Soc.*, **2001**, *123*, 12738-12739.

7. Elia, C.; Elyashiv-Barad, S.; Sen, A.; López-Fernández, R.; Albéniz, A. C.; Espinet, P. *Organometallics*, **2002**, *21*, 4249-4256

8. Tian, G.; Boone, H. W.; Novak, B. M. *Macromolecules* **2001**, *34*, 7656-7663.

9. Hatada, K.; Ute, K.; Tanaka, K.; Imanari, M.; Fujii, N. *Polymer Journal* **1987,** 19, 425-436.

10. Matsuzaki, K.; Kawazu, F.; Kanai, T.; *Makromol. Chem.* **1982**, 183, 185-192.

11. Albéniz, A. C.; Espinet, P.; López-Fernández, R.; Sen, A. *J. Am. Chem. Soc.* **2002**, *124*, 11278-11279.

CHAPTER 3 – LEWIS ACID – MEDIATED COPOLYMERIZATION OF METHYL ACRYLATE AND METHYL METHACRYLATE WITH 1-ALKENES

3.1 – INTRODUCTION

The synthesis of polymers with precise and reproducible structures allows for the controlled adjustment of macroscopic properties of such materials. With the wide number of monomers available for radical polymerization, the ability to control radically initiated polymerization has been an area of extensive research. For example, the microstructure control in radical polymerization of acrylate-based monomers through the use of Lewis acids has been reported.[1-3] The complexation of Lewis acid to the ester functionality has been shown to both increase reactivity of the monomer and affect the tacticity of the resultant polymer.[3] The latter is believed to be due the simultaneous complexation of several monomer units to the Lewis acid resulting in the formation of meso triads upon polymerization, and ultimately an overall increase in isotacticity of the polymer (TABLE 3.1).

An important remaining challenge in polymer synthesis is the copolymerization of polar monomers with simple alkenes. We[4-7] and others[8-10] have reported on the copolymerization of acrylates with ethene and 1-alkenes. The molecular weight and molecular weight distribution of the resultant random copolymers can be regulated using controlled radical polymerization techniques. However, there is little control over polymer tacticity or the amount 1-alkene incorporated into the polymer backbone.

TABLE 3.1 - Radical Homopolymerization of MMA in the presence of $Sc(OTf)_3$[a]

Entry	Monomer	Monomer: $Sc(OTf)_3$	M_W (X 10^{-3})	PDI	Tacticity		
					%mm (isotactic)	%mr	%rr (syndiotatic)
1[3]	MMA	NONE	72.6	1.93	7	35	58
2[3]	MMA	24:1	40.8	1.90	8	39	53
3[3]	MMA	12:1	52.3	2.23	14	46	40
4[b]	MMA	3:1	21.8	1.63	27	41	32
5[b]	MMA	1.5:1	15.3	1.21	28	41	31

[a]60 °C for 18 hours in chlorobenzene [b]Megan Nagel (unpublished results)

The ability to control the latter properties would result in additional control over bulk properties, such as glass transition temperature (T_g) and material toughness. Herein we report the synthesis of copolymers of methyl methacrylate and acrylate with ethene and 1-alkenes in the presence of the Lewis acid, $Sc(OTf)_3$. We demonstrate that only a catalytic amount of $Sc(OTf)_3$ is sufficient to form nearly alternating copolymers in high yield.

3.2 – RESULTS AND DISCUSSION

3.2.1 – COPOLYMERIZATION OF METHYL METHACRYLATE WITH 1-ALKENES

The effect of the addition of $Sc(OTf)_3$ to AIBN-initiated copolymerization of methyl methacrylate (MMA) with ethene and 1-hexene is summarized in TABLE 3.2 In all cases, an increase in 1-alkene incorporation was observed in the presence of $Sc(OTf)_3$. Additionally, this effect becomes greater as the amount of $Sc(OTf)_3$ is increased. For example, comparison of the copolymerization of MMA and ethene in the absence of $Sc(OTf)_3$ to those with the addition of 0.1 eq. and 0.2 eq. of $Sc(OTf)_3$ (versus the MMA), shows the mole percent of ethene incorporated in to the polymer backbone increases from 22 to 27 to 37%, respectively. This then allows for the control of copolymer composition independent of the starting monomer feed ratio. More dramatic is the increase in MMA conversion upon the addition of $Sc(OTf)_3$ to the reaction mixture. In all cases, the MMA conversion more than doubles after the addition of 0.1 equivalents of $Sc(OTf)_3$.

The addition of $Sc(OTf)_3$ during the homopolymerization of MMA results in an increased number of isotactic triads as a consequence of more than one monomer simultaneously coordinating to the scandium center at the growing chain end.[3] The obvious question that arose was whether the enhancement of isotactic triads was maintained in the copolymerization reaction. However, for the copolymers with 1-alkenes, the triad information calculated from integration of the α-methyl resonances in

TABLE 3.2 – Copolymerization of Methyl Methacrylate with 1-Alkenes Using AIBN in the Presence of $Sc(OTf)_3$[a]

Entry	$Sc(OTf)_3$: Monomer	Alkene (psi or g)[b]	Yield (g)	M_w (x 10^{-3})[c]	M_w/M_n[c]	Alkene incorp. (mol %)	MMA Conversion (%)
1	0	Ethene(500)	0.011	152	2.4	22	3.3
2	1:10	Ethene (500)	0.26	245	3.0	27	76
3	1:5	Ethene (500)	0.26	32.3	1.3	37	76
4	0	1-Hexene (3.75)	0.11	49.2	1.3	12	31
5	1:10	1-Hexene (3.75)	0.28	111	2.7	19	63

[a]Reaction Conditions:AIBN, 4 mg; MMA, 3 mmol; PhCl, 5 mL; 60 °C, 18 h. [b] 0.0163 M ethene, 5.0 M 1-hexene [c]By SEC relative to polystyrene standards.

the ^{1}H-NMR spectrum could not be obtained due to overlapping signals from the 1-alkene comonomer now incorporated into the polymer backbone. Therefore, a copolymer was prepared from MMA and C_2D_4, and the ^{1}H NMR spectrum is in FIGURE 3.1. The incorporation of the latter monomer was confirmed by ^{2}D-NMR spectroscopy. From the integration of the α-methyl peaks in the ^{1}H-NMR spectrum, it was clear that the tacticity of the MMA triads in the copolymer was no different than that in PMMA prepared in the absence of $Sc(OTf)_3$ (TABLE 3.3). Presumably, the presence of the 1-alkene units in the copolymer backbone interferes with the simultaneous coordination of several MMA units to the scandium center, a condition necessary for the enhanced formation of isotactic triads.

3.2.2 – COPOLYMERIZATION OF METHYL ACRYLATE AND α - OLEFINS

Unlike MMA, the addition of $Sc(OTf)_3$ during the radical-initiated homopolymerization of methyl acrylate (MA) did not result in polymer microstructure different from the usual atactic structure obtained in the absence of the Lewis acid. Therefore, ^{13}C-NMR spectroscopy was employed to examine the interaction between MA and $Sc(OTf)_3$. As shown in TABLE 3.4, there are small but distinct shifts of the resonances in the presence of $Sc(OTf)_3$. The biggest shift is for the carbon of the carbonyl group: the expected biding site for scandium. These results are similar to those observed for MMA,[3] and once again suggest an interaction between the ester group of the MA and scandium center of $Sc(OTf)_3$.

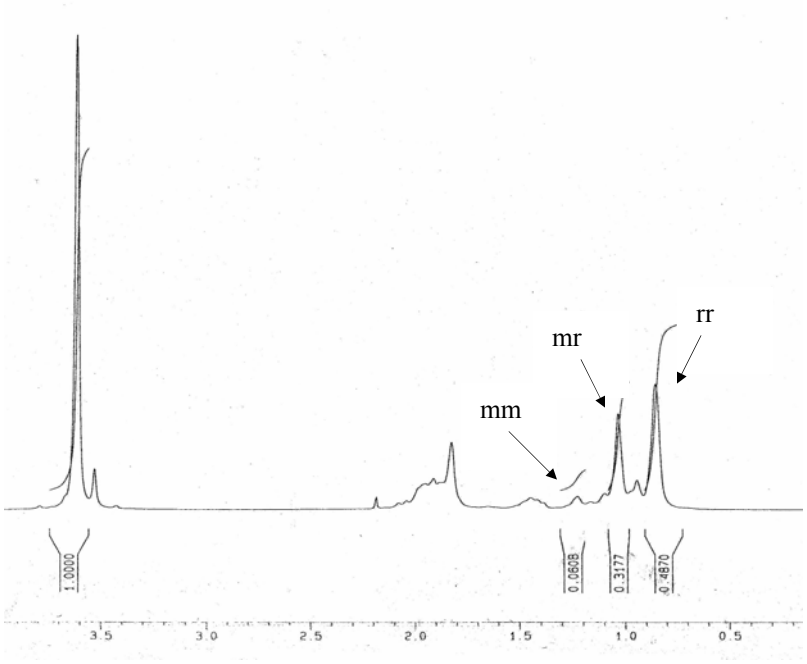

FIGURE 3.1 – ^{1}H NMR of MMA and C_2D_4 Copolymer made in the presence of $Sc(OTf)_3$

TABLE 3.3 – Tacticity of PMMA Segments after Homo- and Copolymerization in the Presence of $Sc(OTf)_3$[a]

Entry	$Sc(OTf)_3$:Monomer	Comonomer	Tacticity[b]		
			% mm	% mr	% rr
1	0	None	7	36	67
2	1 :10	None	18	42	40
3	1 :10	C_2D_4[c]	7	37	68

[a]Reaction Conditions: AIBN, 4 mg; MMA, 3 mmol; PhCl, 5 mL; 60 °C, 18h. [b]Determined by ^{1}H-NMR spectroscopy. [c]C_2D_4, 300 psi.

TABLE 3.4 – Changes in the ^{13}C NMR Chemical Shifts of Methyl Acrylate Upon the Addition of $Sc(OTf)_3$[a]

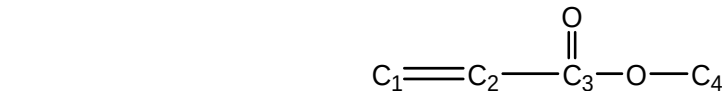

Carbon	MA (ppm)	Added $Sc(OTf)_3$ (ppm)[a]	Δδ (ppm)
1	129.86	131.19	1.34
2	128.65	128.29	-0.36
3	165.66	167.11	1.45
4	51.17	51.72	0.55

[a]MA:$Sc(OTf)_3$ = 10 (molar ratio)

Although tacticity change was not observed in the MA homopolymer obtained in the presence of $Sc(OTf)_3$, the above NMR results suggested that the interaction between the MA and $Sc(OTf)_3$ may still be strong enough to promote the copolymerization of MA with nonpolar 1-alkenes. Our results in this area are summarized in TABLE 3.5. In every case the addition of $Sc(OTf)_3$ resulted in a significant increase of the amount of alkene incorporation. For example, the copolymerization of MA and ethene in the presence of 0.1 mole ratio of $Sc(OTf)_3$ versus MA produced a copolymer containing 47% mole percent of the latter. The ^{13}C-NMR spectrum of this polymer contained five dominant resonances at 176.4 (-C(O)-), 51.8 ($-OCH_3$), 45.7 (-CH-), 32.7 ($-CH_2-$), and 25.8 ppm ($-CH_2-$). These represent the five signals from a perfectly alternating MA-ethene copolymer sequence.[12] Two less intense resonances at 43.6 and 34.8 ppm were also present and are due to consecutive MA units, suggesting some non perfect alternation. Alternating MA/ethene copolymers have been previously reported, but the synthesis requires a stoichiometric amount of a strong Lewis acid such as $AlCl_3$ or BF_3.[13,14] $Sc(OTf)_3$ is a relatively air stable compound that offers much the same result in significantly lower concentrations.

The effect of varying amounts of $Sc(OTf)_3$ was also examined for the copolymerization of MA with ethene. In all cases, the result is increased ethene incorporation into the copolymer, but the level of increase is directly dependent on the amount of $Sc(OTf)_3$ present (FIGURE 3.2). Clearly the results point to the ability to "dial-in" a copolymer composition by simply adjusting the amount of $Sc(OTf)_3$ added to the radically initiated copolymerization.

TABLE 3.5 – Copolymerization of Methyl Acrylate with 1-Alkenes Using AIBN in the Presence of $Sc(OTf)_3$[a]

Entry	MA (g)	$Sc(OTf)_3$: Monomer	Comonomer (psi or g)[b]	Yield (g)	M_w (x 10^{-3})[c]	M_w/M_n[c]	Olefin Incorp. (mol%)	MA Conv. (%)
1	0.31	0	Ethene (500)	0.069	99	1.7	30	20
2	0.31	1:10	Ethene (500)	0.298	132	2.9	47	74
3	0.30	0	Propene (6.5)	0.010	49	1.6	41	1.3
4	0.26	1:10	Propene (6.5)	0.081	238	2.2	46	22
5	0.30	0	1-Hexene (1)	0.010	25	1.6	26	1.2
6	0.31	1:10	1-Hexene (1)	0.064	86	2.1	41	12
7	0.31	0	1-Decene (3.3)	0.18	37	1.4	25	19
8	0.33	1:10	1-Decene (3.3)	0.279	58	2.3	40	41
9	0.33	0	Norbornene (2.9)	0.19	47	1.6	22	22
10	0.32	1:10	Norbornene (2.9)	0.304	36	2.3	33	62

[a]Reaction Conditions: AIBN, 4mg; MA, 3.5 mmol; PhCl, 5mL; 60 °C, 18 h. [b] 0.039 M ethene, 0.121 M propene, 2.0 M 1-hexene, 3.2 M 1-decene, 6.2 M norbornene [c]By SEC relative to polystyrene standards.

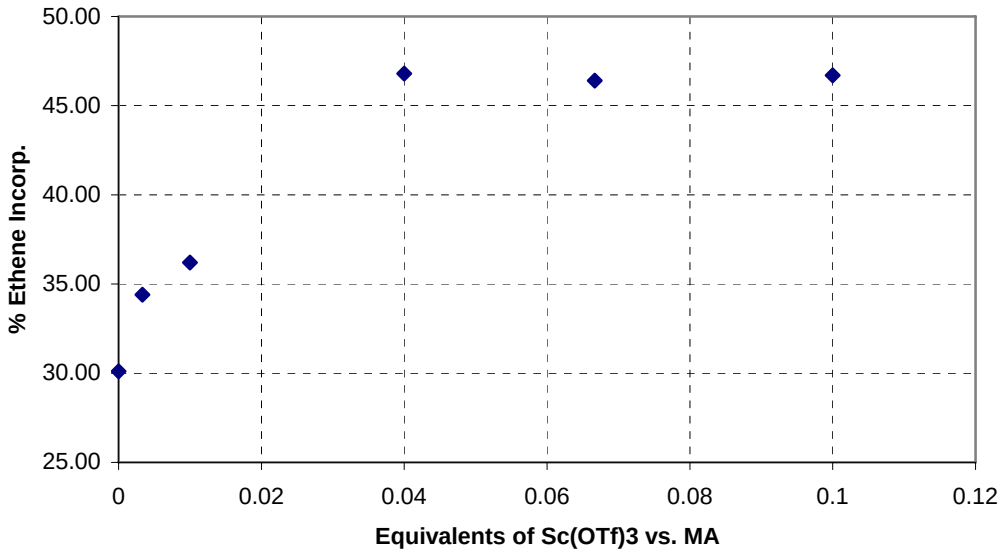

FIGURE 3.2 - Ethene (mol%) in the Copolymer as a Function of the Amount of $Sc(OTf)_3$ Present. MA, 0.70 M, ethene, 500 psi ; AIBN, 4.9 mM; chlorobenzene, 60 °C, 18 h.

As with the MMA copolymerization, the presence of the $Sc(OTf)_3$ also affects the yield of the MA/alkene copolymers obtained. The amount of product from the reaction increases as the amount of $Sc(OTf)_3$ in the system increases (FIGURE 3.3). In FIGURES 3.2 and 3.3, the amount of conversion and incorporation both level off as the amount of $Sc(OTf)_3$ approaches 10% of the MA. At these concentrations, the MA solution has become saturated, and thus adding additional $Sc(OTf)_3$ has little effect on the polymerization properties. As seen from FIGURES. 3.2 and 3.3, it is possible to synthesize a polymer that is nearly alternating in MA and ethene at 67% MA conversion with only 4 mol% of $Sc(OTf)_3$ per MA. The fact that an alternating copolymer can be prepared using such a low $Sc(OTf)_3$:MA ratio suggests facile Sc^{3+} exchange between MA units in the polymer and monomeric MA as shown in FIGURE 3.4.

In all cases it was confirmed by gel permeation chromatography (GPC) that these were in fact true copolymers and not a mixture of two homopolymers. The GPC chromatogram showed only one peak for both the refractive index (RI) and UV detectors. The latter is of course more sensitive to acrylate groups. This indicates a true copolymer over the entire molecular weight distribution range.

3.2.3 – CONTROLLED POLYMERIZATION OF MA AND 1-HEXENE IN THE PRESENCE OF $Sc(OTf)_3$

In the conventional free-radical copolymerization of acrylates with 1-alkenes, there is little control over molecular weight or molecular weight distribution. We[14] and others[15] have reported on controlled copolymerization using the reversible addition-

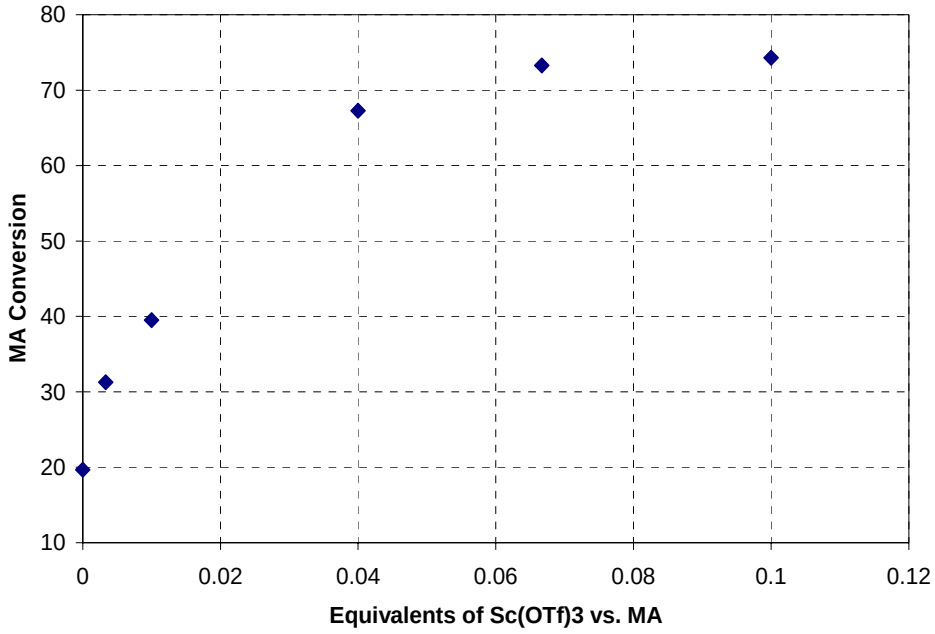

FIGURE 3.3 - MA Conversion as a Function of the Amount of $Sc(OTf)_3$ Present. MA, 0.70 M, ethene, 500 psi ; AIBN, 4.9 mM; chlorobenzene, 60 °C, 18 h.

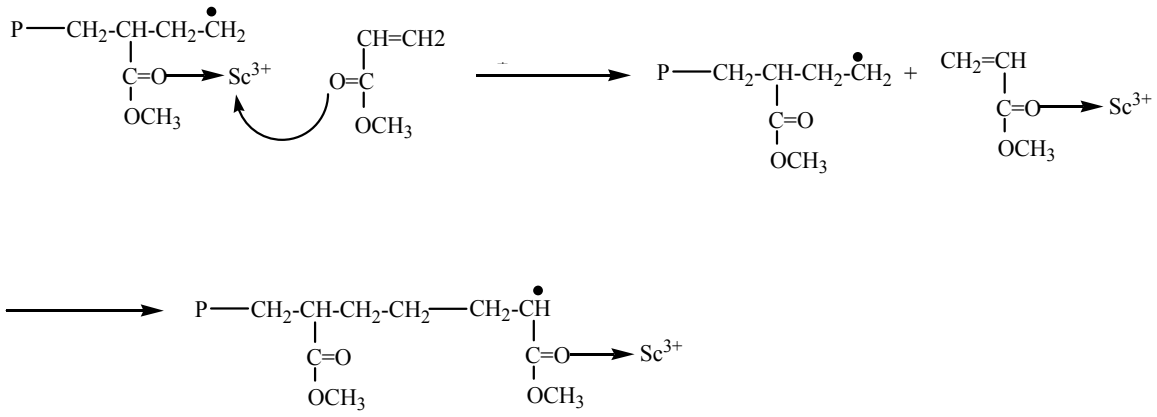

FIGURE 3.4 – Scheme of the facile exchange between the Sc^{3+} and the carbonyl of the incoming methyl acrylate monomer.

fragmentation transfer (RAFT) technique. RAFT polymerization was also found to control the alternating copolymerization of MA and ethene in the presence of the Lewis acid, $AlCl_3$.[14]

We have examined the effect of RAFT agent on the AIBN-initiated copolymerization of MA with 1-hexene in the presence of $Sc(OTf)_3$. The RAFT agent, 1-pyrrolcarbodithioate, was chosen since it has been shown to be effective for copolymerizations in the presence of $AlCl_3$. As shown in FIGURE. 3.5, the copolymerization displays first-order kinetics. Additionally, there is initially a linear increase in molecular weight with conversion (FIGURE 3.6). However, the line curves at higher conversions and there is a simultaneous increase in polydispersity of the copolymer obtained. This suggests that the propagating radical is not long-lived and the reaction does not meet the criteria for "living" polymerizations.

The results from increasing the amount of RAFT agent present during the copolymerization of MA with 1-hexene are summarized in TABLE 3.6. Both the molecular weight and molecular weight distribution decrease with increasing concentration of the RAFT agent. For example, as the RAFT/AIBN molar ratio increases from 0 to 5 to 10, the M_w decreases from 209,000 to 140,000 to 70,000, and the molecular weight distribution decreases from 2.7 to 2.2 to 1.7. Thus, although some control is observed, the copolymerizations are not as well behaved as that observed without $Sc(OTf)_3$. One can speculate that $Sc(OTf)_3$ interferes with the functioning of the RAFT agent. The observation that the amount of 1-hexene incorporated into the copolymer decreases with increasing concentration of the RAFT agent provides indirect support for this hypothesis. Nevertheless, the amount of 1-alkene incorporated is

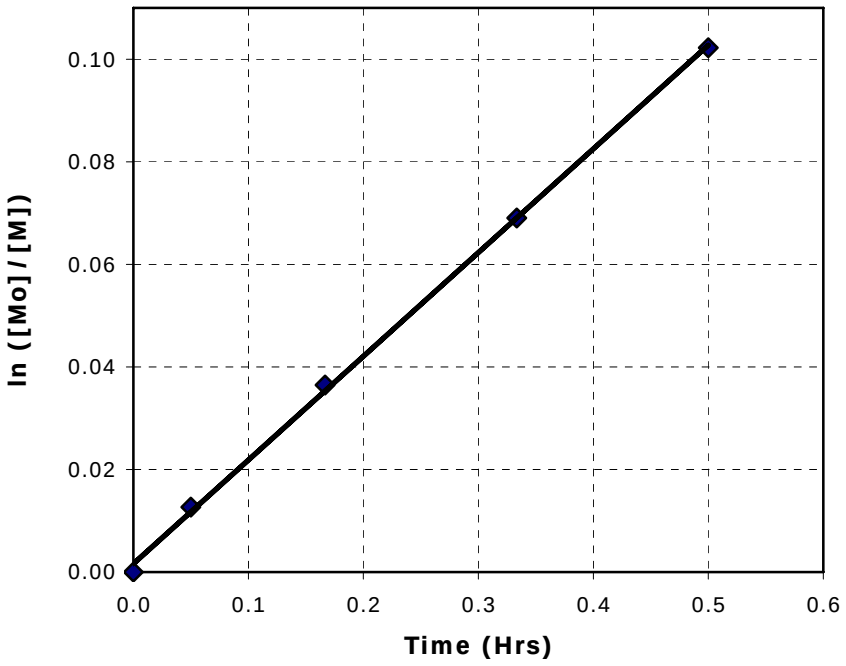

FIGURE 3.5 - First Order Kinetic Plot for the Copolymerization of MA with 1-Hexene. MA, 2.6 M; 1-hexene, 2.7 M; RAFT, 8.3 mM; AIBN, 0.83 mM; Chlorobenzene, 60°C.

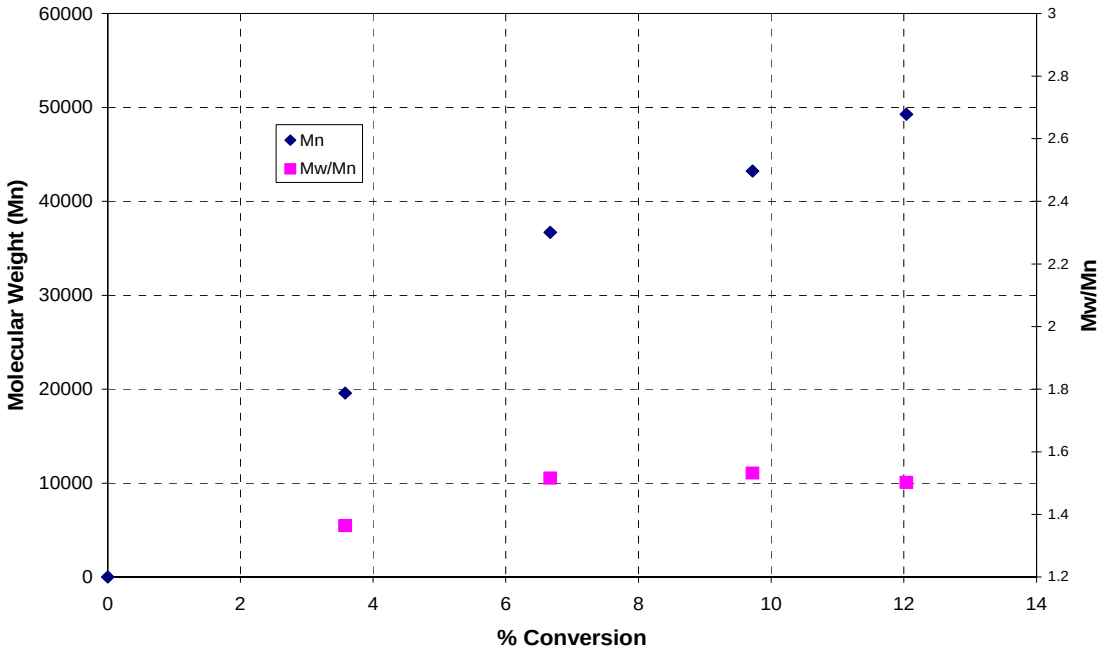

FIGURE 3.6 - Dependence of Molecular Weight (M_n) and Molecular Weight Distribution (M_w/M_n) on Overall Conversion in the Copolymerization of Methyl Acrylate with 1-Hexene. MA, 2.6 M; 1-hexene, 2.7 M; RAFT, 8.3 mM; AIBN, 0.83 mM; Chlorobenzene, 60°C.

TABLE 3.6 – RAFT Copolymerization of Methyl Acrylate and 1-Hexene with $Sc(OTf)_3$ / AIBN[a]

Entry	RAFT/AIBN (molar ratio)	M_w (x 10^{-3}) [b]	M_w/M_n [b]	1-alkene (mol %)	MA Conversion (%)
1	0	209	2.8	30	71
2	5	140	2.2	27	37
3	10	70	1.7	25	6.0

[a]Reaction Conditions: MA, 2.6 M; 1-hexene, 2.7 M; AIBN, 0.83 mM; chlorobenzene, MA:$Sc(OTf)_3$ = 10 , 60°C, 18 h. [b]By SEC relative to polystyrene standards.

significantly greater with the introduction of $Sc(OTf)_3$ into the system. A maximum of 12 mole% 1-hexene incorporation was reported for controlled copolymerization with a RAFT/AIBN ratio of 10 without $Sc(OTf)_3$.[14] With $Sc(OTf)_3$, and a RAFT/AIBN ratio of 10, the mole % of 1-hexene is 25.

3.3 – CONCLUSIONS

The addition of the Lewis acid, $Sc(OTf)_3$, to AIBN-initiated copolymerizations of both MA and MMA with 1-alkenes results in increased reaction rate and increased incorporation of the latter monomer into the polymer backbone. As little as 4 mol% of the Lewis acid is effective in forming a nearly alternating copolymer of MA and ethene at 67% MA conversion. This procedure allows for the control of copolymer composition independent of the starting monomer feed ratio.

3.4 – EXPERIMENTAL PROCEDURES

3.4.1 – MATERIALS

All chemicals and reagents were obtained from Aldrich unless otherwise stated. Methyl acrylate (MA, 99%), methyl methacrylate (MMA, 99%), and 1-hexene were vacuum distilled from CaH_2 and stored under N_2. 2,2'-Azobis(isobutyronitrile) (AIBN, 98%) and scandium(III)trifluoromethanesulfonate ($Sc(OTf)_3$, 97%, Strem Chemicals) were used as received. The RAFT agent, benzyl 1-pyrrolcarbodithioate, was synthesized according to the literature.[11] 1H NMR (CDCl3, ppm): 4.62 (s, 2H, CH_2PH), 6.35 (m, 2H, pyrrole), 7.40 (m, 5H, CH_2Ph), 7.73 (m, 2H, pyrrole).

3.4.2 – INSTRUMENTATION

Gas chromatography analysis was obtained on an Agilent 5890 Series II GC using a RTX-5 split capillary column (Restek) connected to an FID detector. NMR spectra were recorded on a Bruker 300-DPX spectrometer. Chemical shifts were referenced to $CDCl_3$. Molecular weights and molecular weight distributions were determined on a Shimadzu gel permeation chromatography (GPC) chomatograph containing a three column bed (styragel HR 7.8 x 300mm columns with 5μm bead size: 100-5,000, 500-30,000, and 2,000-4 x 10^6 Da), Shimadzu RID-10A differential refractometer, and Shimadzu SPD-10A tunable absorbance detector (254nm). GPC samples were run in

chloroform at a flow rate of 1mL/min at 35°C and calibrated against polystyrene standards. Analysis was done using EZSTART 7.2 software.

3.4.3 – SYNTHESIS OF HOMO- AND COPOLYMERS

In a typical experiment, (Table 1, entry 2) in a N_2 filled dry glovebox, a glass-lined Parr high pressure reactor was charged with solvent (5 mL), AIBN (0.024 mmol), MMA (3 mmol), and 0.3 mmol of $Sc(OTf)_3$. The vial was sealed, removed from the glovebox, and filled with ethene to 500 psi. The reaction was allowed to stir in a 60 °C oil bath for 18 h. At the end of this period, the reaction was cooled and vented, and the polymer was precipitated with a large excess of methanol. The polymer was collected by vacuum filtration and dried under high vacuum for 24 h. For those reactions which did not require a Parr reactor, the polymerizations were carried out in a 20 mL scintillation vial. Polymer composition was determined by integration of the methyoxy proton resonances versus integration over the total aliphatic region.

3.4.4. – SYNTHESIS OF METHYL ACRYLATE / 1-HEXENE COPOLYMERS BY RAFT POLYMERIZATION

In a N_2 filled dry glovebox, a 20 mL scintillation vial with a magnetic stir bar was charged with chlorobenzene (4 mL), MA (11.6 mmmol), 1-hexene (11.9 mmmol), AIBN (4.1 μmol), and the appropriate amount of 1-pyrrolcarbodithioate (RAFT agent). The

reaction was allowed to stir at 60 °C. After 18 h, the samples were cooled to room temperature and worked up as described above.

3.4.5 – KINETIC STUDY OF METHYL ACRYLATE / 1-HEXENE RAFT COPOLYMERIZATION IN THE PRESENCE OF $Sc(OTf)_3$

In a N_2 filled dry glovebox, a reaction vessel with a magnetic stir bar was charged with chlorobenzene (10 mL), MA (58.1 mmol), 1-hexene (59.5 mmol), benzyl 1-pyrrolcarbodithiate (0.18 mmol), and AIBN (0.018 mmol). The reaction vessel was then placed in an oil bath at 60° C. Samples were taken with a syringe and used for GC and GPC analysis to determine monomer conversion, molecular weight and molecular weight distribution.

3.5 – REFERENCES

1. Otsu, T.; Yamada, B.; Imoto, M. *J. Macromol. Chem.* **1966,** *1,* 61.
2. Okazawa, S.; Hirai, H. Makishima, S. *J. Polym. Sci. A1*, **1969,** 1, 1039.
3. Isobe, Y.; Nakano, T.; Okamoto, Y. *J. Polym. Sci., Part A: Polym. Chem.* **2001**, *39*,1463.
4. Liu, S. H.; Elyashiv, S.; Sen, A. *J. Am. Chem. Soc.* **2001**, *123*, 12738.
5. Elyashiv, S.; Greinert, N.; Sen, A. *Macromolecules* **2002**, *35*, 7521.
6. Gu, B.; Liu, S.; Leber, D.; Sen, A. *Macromolecules* **2004,** *37*, 51425
7. Liu, S.; Sen, A. *J. Polym. Sci., Part A: Polym. Chem.* **2004**, *42*, 6175.
8. Tian, G.; Boone, H. W.; Novak, B. M. *Macromolecules*, **2001**, *34*, 7656.
9. Venkatesh, R.; Klumperman, B. *Macromolecules* **2004**, *37*, 1226.
10. Vankatesh, R.; Harrison, S.; Haddleton, D. M.; Klumperman, B. *Macromolecules* **2004,** *37*, 4406.
11. Chiefari, J.; Mayadunne, R. T. A.; Moad, C. L.; Moad, G.; Rizzardo, E.; Postma, A.; Skidmore, M. A.; Thang, S. H. *Macromolecules* **2003**, *36*, 2273.
12. Logothetis, A. L.; McKenna, J. M. *J. Polym. Sci., Polym.Chem. Ed.* **1978**, *16*, 2797.
13. Logothetis, A. L.; McKenna, J.M. *J. Polym. Sci., Polym. Chem. Ed.* **1977**, *15*, 1431.
14. Liu, S.; Gu, B.; Rowlands, H.A.; Sen, A. *Macromolecules* **2004,** *37*, 7924.
15. Venkatesh, R.; Staal, B.; Klumperman, B. *Chem Commun* **2004**, *13*, 1554.

CHAPTER 4 – FORMATION AND DECOMPOSITION OF PALLADIUM-ALKYL COMPLEXES WITH AN ESTER GROUP α TO THE METAL CENTER

4.1– INTRODUCTION

There is great current interest in the copolymerization of acrylates and non-polar α-olefins because of the wide range of properties these materials are expected to exhibit.[1] Radical methods, including controlled radical polymerization techniques, have been reported for such copolymerizations, producing polymers with defined molecular weights and molecular weight distributions.[2] Recently, we also reported control of the comonomer composition for radically initiated copolymerization in the presence of Lewis acids.[3] However, by radical methods, consecutive α-olefin units are rarely observed along the polymer backbone. This prohibits the maximum amount of α-olefin incorporation achieved by these methods from exceeding fifty mole percent.

Early transition metal, Zeigler-Natta-type, catalysts are well known for their ability to readily homopolymerize α-olefins, but they are poisoned in the presence of heteroatoms, including oxygen.[4] This has put the focus on the less oxophilic late-transition metals as catalysts for the copolymerization of acrylates and α-olefins with greater than fifty mole percent α-olefin incorporation. There have been numerous attempts of this type reported, but unfortunately there are only a few successful examples that have been shown to proceed through an insertion-type mechanism.[5]

Another more abundant, yet less note-worthy, class of late-transition metal compounds have also been shown to copolymerize acrylates and non-polar monomers, but the polymer produced from these compounds is acrylate rich, resembling those made by free-radical methods.[6] In none of these cases can an insertion-type mechanism be confirmed. In fact, for neutral palladium complexes, homolytic cleavage of the palladium-alkyl bond following a single acrylate insertion has been shown to occur and subsequently initiate polymerization in the presence of excess methyl acrylate.[7] This can be largely attributed to the fact that, for electronic reasons, methyl acrylate prefers 2,1 insertion, and the radical formed upon homolytic cleavage is identical to the propagating acrylate species in free-radical polymerization (FIGURE 4.1).[8] Furthermore, this metal-alkyl bond homolysis is know to occur on the same timescale as β-hydrogen elimination / readdition steps.[9]

To simplify the design of future catalyst systems, it is essential to a gain greater understanding of the barriers that currently prohibit the successful insertion copolymerization of acrylates and α-olefins, specifically the formation of radicals, even in low concentrations. Herein we use a general, neutral palladium system to study the decomposition of the palladium-alkyl bond following a single acrylate insertion.

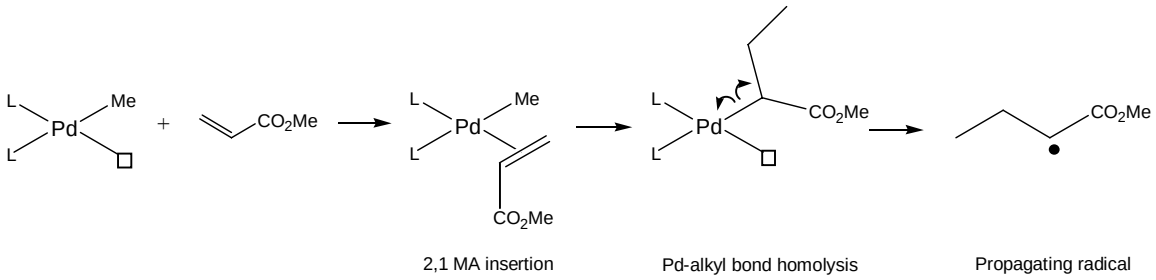

FIGURE 4.1 – Pd-C bond homolysis for a general palladium system following a single insertion of methyl acrylate.

4.2 RESULTS AND DISCUSSION

4.2.1 – COMPLEX SYNTHESIS AND DECOMPOSITION

To simulate the single insertion of methyl acrylate into a palladium-methyl bond, a palladium complex was synthesized from bis(dibenzylideneacetone) palladium(0) ($Pd_2(dba)_3$) and two equivalents *per palladium* of triphenylphosphine (PPh_3). To this mixture, one equivalent of the alkyl bromide, methyl 2-bromobutyrate was added. The oxidative addition between the methyl 2-bromobutyrate and the palladium compound should provide a well-defined complex analogous to the single insertion product of methyl acrylate into the palladium alkyl bond of a neutral palladium complex (FIGURE 4.2). Almost immediately following the addition of the methyl 2-bromobutyrate at room temperature, a yellow precipitate formed, and ^1H NMR showed conversion of the methyl 2-bromobutyrate to two new products. The major product was identified as methyl crotonate (16% overall) and a secondary product was methyl butyrate (2.5%). The yellow precipitate was confirmed by x-ray crystallography to be $PdBr_2(PPh_3)_2$ (FIGURE 4.3).

Based on the decomposition products it is clear that the palladium-alkyl complex is unstable, and we have proposed two distinct decomposition pathways following the oxidative addition. The first of these is β-hydrogen elimination to give methyl crotonate. The second is the homolytic cleavage of the palladium-alkyl bond to give active radicals.

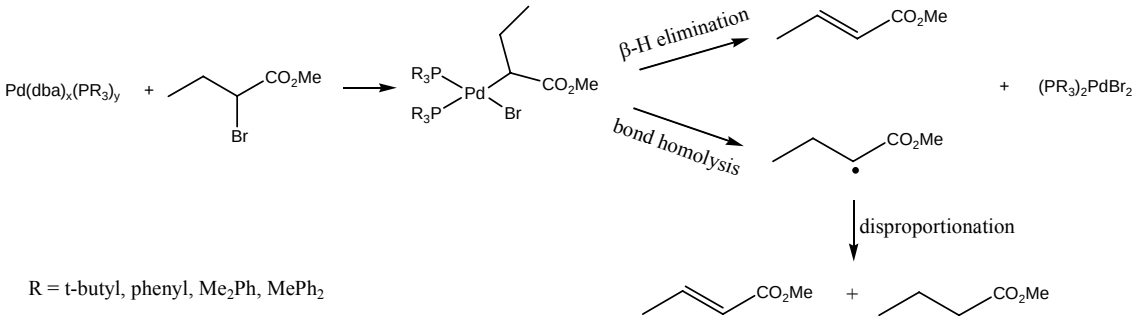

FIGURE 4.2 – Formation and decomposition of palladium complex following oxidative addition of methyl 2-bromobutyrate.

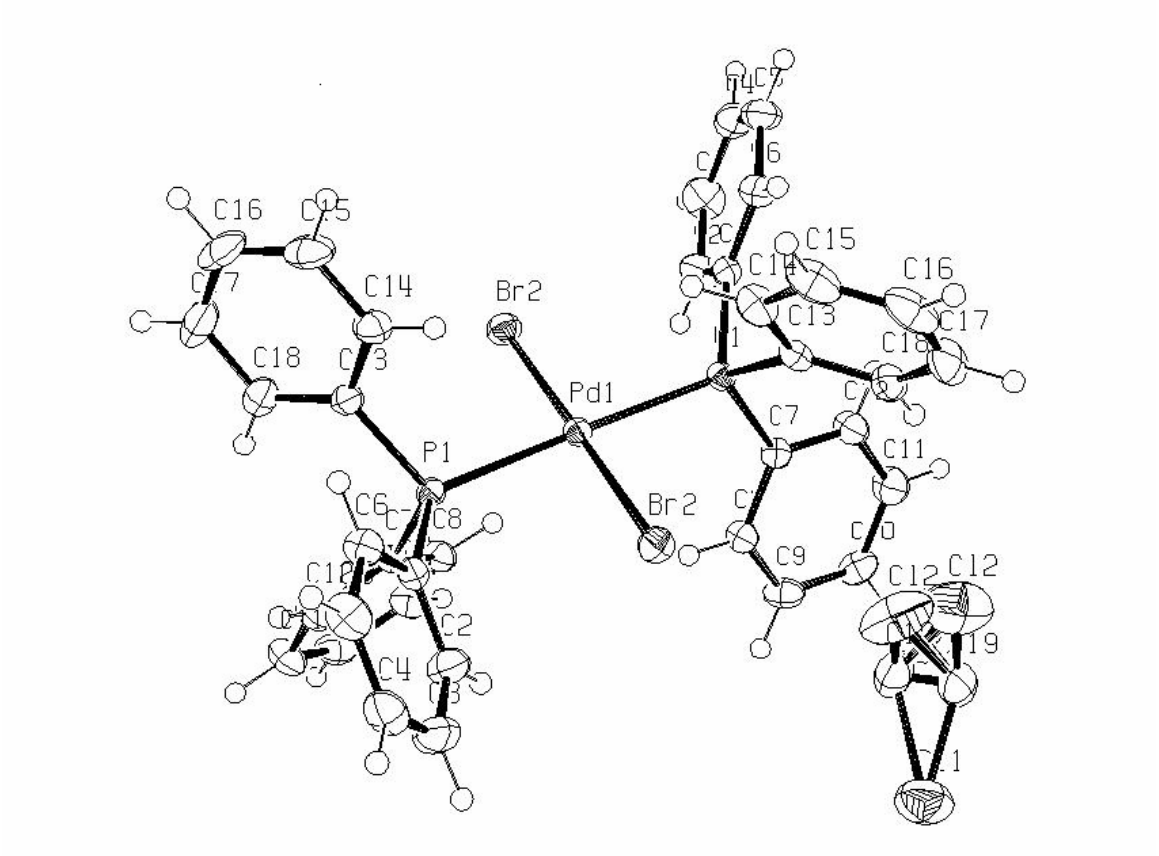

FIGURE 4.3 - ORTEP diagram for the X-ray crystallography structure determination of #19, mlm4 dibromobis(triphenylphosphine)palladium(II) [$PdBr_2(PPh_3)_2$]

These radicals then undergo disproportionation to give both methyl butyrate and methyl crotonate. In the presence of excess methyl acrylate, homopolymerization ensues to give atactic poly(methyl acrylate) (7.0% yield, M_w = 489,000, PDI = 1.6).

In an attempt to stifle the major decomposition pathway, β-H elimination, the reaction was repeated replacing methyl 2-bromobutyrate with methyl α-bromophenylacetate, which does not contain a β-hydrogen. Upon oxidative addition of methyl α-bromophenylacetate with the palladium-phosphine complex, the complex was again found to entirely decompose. In this case, the decomposition occurred only by homolytic cleavage of the palladium-alkyl bond. By ^{1}H NMR, the decomposition product was confirmed to be the dimeric product formed from the combination of the cleaved methylphenylacetate radicals as seen in FIGURE 4.4 (35% conversion of the methyl α-bromophenylacetate). Again, in the presence of excess methyl acrylate, polymerization occurs (27% yield, M_w = 91,000, PDI = 2.0). Because all of the palladium-alkyl bonds are forced to decompose by bond homolysis, an increased number of radicals are formed. This both increased the conversion, and significantly decreased the molecular weight of the resultant MA polymer.

4.2.2 – VARYING THE PHOSPHINE LIGAND

Only 18.5% of the starting material was converted to the decomposition products when using PPh_3 as the ligand, and the remaining 80% of the methyl 2-bromobutyrate

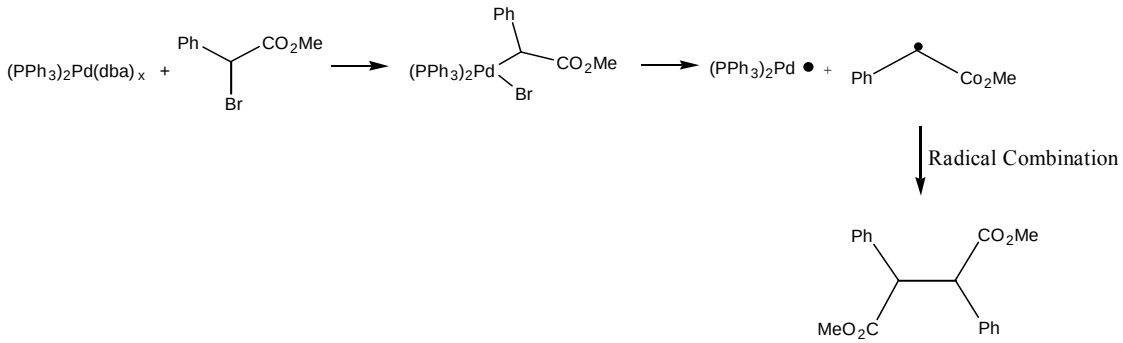

FIGURE 4.4 Formation and decomposition of palladium complex following oxidative addition of methyl α-bromophenylacetate.

was left unreacted. We attribute this to a lack of active palladium compound formed from the PPh_3 and $Pd_2(dba)_3$. From ^{31}P NMR it was clear that only a small portion of the free phosphine ligand (δ = -6.95ppm) was converted to the active palladium compound (δ = 25.88 ppm) prior to the addition of the alkyl bromide. Also, the active species that was formed did not produce a stable metal-alkyl complex following the oxidative addition. This led us to employ three different phosphine ligands, tri-t-butylphosphine ($P(t\text{-butyl})_3$), methyldiphenylphosphine ($PMePh_2$), and dimethylphenylphosphine (PMe_2Ph) which all have various electronic and steric properties (TABLE 4.1).

For each of these three ligands, four equivalents were added to $Pd_2(dba)_3$. This was again followed by the addition of one equivalent of methyl 2-bromobutyrate to the new palladium complex. With each of these ligands, nearly quantitative amounts of the active palladium species was formed, and the free ligand peak was completely shifted in the ^{31}P NMR upon addition to the palladium compound. Finally, nearly all of the methyl 2-bromobutyrate was consumed for each reaction. In all of the cases, we were still unable to observe the formation of a stable palladium-alkyl complex at room temperature. The decomposition products, methyl crotonate and methyl butyrate were confirmed by ^1H NMR and gas chromatography. Polymerization was also observed for each system in the presence of excess methyl acrylate (TABLE 4.2).

Although the different properties of the ligands did not have an effect on the long-term stability of the palladium-alkyl complexes, the modes of decomposition did vary dramatically depending on the ligand used (TABLE 4.3). For example, based on the decomposition products, the ligand with the largest steric bulk and electronic

TABLE 4.1 Steric and Electronic Contributions of Selected Phosphine Ligands[10]

Ligand	**Steric Contribution** Cone Angle (θ, deg)	**Electronic Contribution** Electronic Parameter (ν)
$P(Me)_2Ph$	122	2065.3
$P(Me)Ph_2$	136	2067.0
PPh_3	145	2068.9
$P(t\text{-butyl})_3$	182	2056.1

TABLE 4.2 Homopolymerization of Methyl Acrylate[a]

Entry	Ligand	Initiator	MA (g)	Yield	MW (X 10^{-3})	Mw/Mn
1	PPh_3	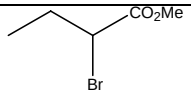	1.05	6.9%	489	1.6
2	PPh_3	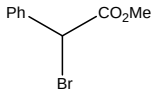	1.02	27%	91	2.0
3	$P(t\text{-butyl})_3$	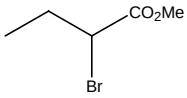	1.05	21%	45	1.4
4	$P(Me)_2Ph$	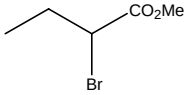	1.04	15%	65	1.5
5	$P(Me)Ph_2$	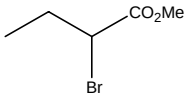	1.13	56%	125	1.9

[a]Reaction Conditions: $Pd_2(dba)_3$, 15mg, 0.016mmol; Initiator, 6mg, 0.032mmol, CH_2Cl_2, 1.5 mL; room temperature, 18 h.

TABLE 4.3 Decomposition Products with Various Phophine Ligands[a]

Entry	Ligand	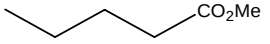 (μmol) / (yield)	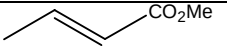 (μmol) / yield
1	$P(Me)_2Ph$	5.1 (14%)	30 (86%)
2	$P(Me)Ph_2$	15 (43%)	17 (49%)
3	PPh_3	0.9 (2.5%)	6.0 (16%)
4	$P(t\text{-butyl})_3$	0.7 (2.1%)	32 (90%)

[a] Reaction Conditions: $Pd_2(dba)_3$, 15mg, 0.016mmol; ligand, 0.65 mmol; methyl 2-bromobutyrate, 6mg, 0.032mmol, CH_2Cl_2, 1.5 mL; room temperature, 18 h.

contribution, P(t-butyl)$_3$, strongly preferred decomposition by β-hydrogen elimination. On the contrary, the sterically smaller and less basic ligand, $PMePh_2$ decomposed nearly entirely by homolysis of the palladium-alkyl bond. Finally, the dimethylphenylphosphine (PMe_2Ph) ligand used has a similar cone angle as the $PMePh_2$, but yet the difference in electronic properties has a dramatic effect on the decomposition pathway. From these three ligands, it appears that as the basicity of the ligand increases, the fewer radicals that are generated in the system.

Additionally, when these experiments were repeated in the presence of excess methyl acrylate, the molecular weight of the polymers formed also reflects this trend. As the number of radicals produced in the system decreased, the molecular weight of the polymer increased.

Because the complex formed using the P(t-butyl)$_3$ ligand decomposed almost solely by β-hydrogen elimination, the methyl 2-bromobutyrate was once again replaced with methyl α-bromophenylacetate to eliminate the major decomposition pathway. However, there was still no formation of a stable complex, and the complex decomposed by metal-alkyl bond homolysis, forming the radical combination product (12% conversion of the methyl α-bromophenylacetate).

As was observed with PPh_3, the final palladium complex formed with each of the other phosphine ligands used is also $[PdBr_2(PR_3)_2]$. This was confirmed by comparing the ^{31}P NMR signals of standard compounds synthesized from $(PhCN)_2PdBr_2$ and the appropriate ligand (P(t-butyl)$_3$, $PMePh_2$, or PMe_2Ph) versus the signal from the reaction mixture following the oxidative addition of methyl 2-bromobutyrate.

4.2.3 – INCREASING THE AMOUNT OF LIGAND PRESENT

In the previous experiments, two equivalents of ligand per palladium were added to the system, followed by oxidative addition of methyl 2-bromobutyrate. Increasing the amount of ligand present should have an overall effect on the decomposition products. For example, when excess ligand is present, the amount of decomposition that occurs by β-hydrogen elimination should decrease because the free ligand that is now present in the reaction mixture creates a competition for the vacant coordination site needed for β-hydrogen elimination to occur.

This is in fact what we observed (TABLE 4.4). The palladium complex formed in the presence of two equivalents of $P(Me)_2Ph$ and one equivalent of methyl 2-bromobutyrate decomposes by β-hydrogen elimination more than 50% of the time. When the reaction is repeated in the presence of more than seven equivalents of ligand, the decomposition shifts to almost solely palladium-alkyl bond homolysis. The same trend also occurs with PPh_3.

When the experiment is repeated using an excess of the bulky $P(t\text{-butyl})_3$ ligand, there does not appear to be a significant change in the ratio of decomposition products. This can be explained by sterics. The free $P(t\text{-butyl})_3$ ligand present in the reaction mixture is sterically too large to engage in competition for the vacant site on the palladium, and the decomposition continues to occur almost entirely by β-hydrogen elimination.

TABLE 4.4 Decomposition Products with Various amounts of Ligand Present[a]

Entry	Ligand	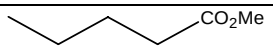 % yield	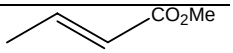 % yield
1	2 eq. $P(Me)_2Ph$	24	76
2	7.5 eq. $P(Me)_2Ph$	48	52
3	2 eq. PPh_3	2.5	16
4	4 eq. PPh_3	28	34
5	2 eq. $P(t\text{-butyl})_3$	2.1	90
6	4 eq. $P(t\text{-butyl})_3$	4.3	60

[a] Reaction Conditions: $Pd_2(dba)_3$, 15mg, 0.016mmol; methyl 2-bromobutyrate, 6mg, 0.032mmol; CH_2Cl_2, 1.5 mL; room temperature, 18 h.

4.3 – CONCLUSIONS

We've again demonstrated the instability of the palladium-alkyl bond where there is an ester group α to the metal center. A similar trend was observed for a variety of phosphine ligands. These palladium-phosphine complexes decomposed by two distinct pathways, β-hydrogen elimination and palladium alkyl bond homolysis. Clearly, there is a correlation between the ligand employed in the system and the preferred mode of decomposition. The generation of radicals in other late transition metal systems has plagued the development of successful catalysts for the insertion polymerization of acrylate and copolymerization with nonpolar alkenes. From this work, it appears that the more basic the ligand that is employed, the less likely that radicals will be generated. Yet, decomposition may still occur by β-hydrogen elimination. The steric contribution of the ligand showed little overall effect on the decomposition.

4.4 – EXPERIMENTAL PROCEDURES

4.4.1 – MATERIALS AND GENERAL CONSIDERATIONS

All manipulations involving air/moisture sensitive compounds were carried out either in a dry N_2 glovebox, or under N_2, using Schlenk techniques. The dichloromethane was distilled, degassed and stored over molecular sieves. Methyl acrylate (MA, 99%) was received from Aldrich, vacuum distilled from CaH_2 and stored under N_2. The methyl 2-bromobutyrate, methyl crotonate and methyl butyrate (Aldrich) were used as received. The palladium compounds and all of the phosphine ligands were purchased from Strem and used as received. Methylene chloride–d_2 was received from Cambridge Isotope Laboratories and used directly from one gram ampoules. Pentachloroethane was obtained from Lancaster Laboratories and was used as an internal standard for quanitative analysis using GC.

4.4.2 – INSTRUMENTATION

Quantification of methyl butyrate and methyl crotonate, and methyl 2-bromobutyrate was done using gas chromatography on an Agilent 5890 Series II GC using a RTX-5 split capillary column (Restek) connected to an FID detector. With an injector temperature of 250°C, the sample was heated from 60° to 120°C at a ramp rate of 4 °C/minute. 1-D ^{1}H-NMR and ^{31}P NMR spectra were recorded on a Bruker DPX-300 (300 MHz) or Bruker AMX-360 (360 MHz) spectrometer. ^{1}H NMR chemical shifts are

reported in parts per million (ppm) relative to residual protiated solvent (CD_2Cl_2, 5.32 ppm). Polymer molecular weights and molecular weight distributions were determined on a Shimadzu gel permeation chromatography (GPC) chomatograph containing a three column bed (styragel HR 7.8 x 300mm columns with 5μm bead size: 100-5,000, 500-30,000, and 2,000-4 x 10^6 Da), Shimadzu RID-10A differential refractometer, and Shimadzu SPD-10A tunable absorbance detector (254nm). GPC samples were run in tetrahydrofuran at a flow rate of 1mL/min at 35°C and calibrated against polystyrene standards. Analysis was done using EZSTART 7.2 software.

4.4.3 – SYNTHESIS OF [PdBr(CHEtC(O)OMe)(PR_3)$_2$]

For example, in a scintillation vial, bis(dibenzylideneacetone) palladium(0) (15 mg, 0.016 mmol) as dissolved in approximately 1.5 mL of dichloromethane, making a dark purple solution. Four equivalents of triphenylphosphine (17 mg, 0.065 mmol) were added to this solution at room temperature. Upon addition of the ligand, the solution changed color to slightly yellow. This solution was stirred for at least 10 minutes before one equivalent per palladium of methyl 2-bromobutyrate was added by microsyringe (3.8 μL, 0.033 mmol). This solution was stirred for several hours at room temperature before it was analyzed. This procedure was reproduced with tri-t-butylphosphine, methyldiphenylphosphine, and dimethylphenylphosphine.

4.4.4 ADDITION OF METHYL α-BROMOPHENYLACETATE TO PALLADIUM COMPLEX

In a scintillation vial, bis(dibenzylideneacetone) palladium(0) (15 mg, 0.016 mmol) as dissolved in approximately 1.5 mL of dichloromethane, making a dark purple solution. Four equivalents of either triphenylphosphine (17 mg, 0.065 mmol) or tri-t-butylphosphine (13mg, 0.065 mmol) were added to this solution at room temperature. This solution was stirred for at least 10 minutes before the addition of methyl α-bromophenylacetate (8 mg, 0.035 mmol). This mixture was stirred for several hours at room temperature before analysis. From ^{1}H NMR, a portion of the methyl α-bromophenylacetate was converted to the dimeric radical combination product: ^{1}H NMR (CD_2Cl_2, 360 MHz, ppm) 7.35 (m, 10H, C_6H_5CH-) 4.45 and 4.32 (s, 1H each, C_6H_5CH-) and 3.45 (s, 6H, -OCH_3).

4.4.5 SYNTHESIS OF $[PdBr_2(PR_3)_2]$

The bis(benzonitrile)palladium(II) dibromide was prepared according to the literature.[11] In a scintillation vial, bis(benzonitrile)palladium(II) dibromide (10 mg, 0.0211 mmol) and 2 equivalents of phosphine ligand were added and dissolved in benzene-d_6. This solution was allowed to stir at room temperature for approximately one hour. ^{31}P NMR (C_6D_6, 360 MHz): $PdBr_2(PPh_3)_2$, 24.9; $PdBr_2(P(t\text{-}butyl_3)_2$, 87.5 ppm; $PdBr_2(PMePh_2)_2$, 24.3 ppm; $PdBr_2(PMe_2Ph)_2$, 26.5 ppm.

4.4.6 – HOMOPOLYMERIZATION OF METHYL ACRYLATE

The above procedure was repeated to make the palladium complex, but before the addition of the methyl 2-bromobutyrate, approximately one gram of methyl acrylate was added to the solution. The reaction mixture was allowed to stir in the dark at room temperature for 18 hours before precipitating the resultant polymer in a large excess of methanol. The polymer was collected by vacuum filtration and dried under high vacuum for 24 h.

TABLE 4.5 - Sample and crystal data for $[PdBr_2(PPh_3)_2]$ mlm4 .

Identification code	mlm4 $[PdBr_2(PPh_3)_2]$	
Empirical formula	C37 H30 Br2 Cl3 P2 Pd	
Formula weight	909.12	
Temperature	143(2) K	
Wavelength	0.71073 Å	
Crystal size	0.33 x 0.32 x 0.10 mm	
Crystal habit	yellow brick	
Crystal system	Monoclinic	
Space group	C2/c	
Unit cell dimensions	a = 12.237(7) Å	α= 90°
	b = 14.458(8) Å	β= 92.702(10)°
	c = 20.184(12) Å	γ = 90°
Volume	3567(4) $Å^3$	
Z	4	
Density (calculated)	1.693 g/cm^3	
Absorption coefficient	3.101 mm^{-1}	
F(000)	1796	

TABLE 4.6 Data collection and structure refinement for $[PdBr_2(PPh_3)_2]$ mlm4.

Diffractometer	CCD area detector
Radiation source	fine-focus sealed tube, MoK
Generator power	1600 watts (50 kV, 32mA)
Detector distance	5.8 cm
Data collection method	phi and omega scans
Theta range for data collection	2.02 to 28.39°
Index ranges	$-16 \leq h \leq 16$, $-19 \leq k \leq 18$, $-26 \leq l \leq 26$

TABLE 4.7 Atomic coordinates and equivalent isotropic atomic displacement parameters ($Å^2$) for $[PdBr_2(PPh_3)_2]$ mlm4.

U(eq) is defined as one third of the trace of the orthogonalized U_{ij} tensor.

	x	y	z	U(eq)
Br2	1.176849(17)	0.253793(13)	0.700237(11)	0.02706(7)
C1	0.98111(16)	0.22807(13)	0.57236(10)	0.0212(4)
C2	1.05377(18)	0.29339(16)	0.54894(11)	0.0333(5)
C3	1.1116(2)	0.27613(19)	0.49315(13)	0.0405(5)
C4	1.09869(19)	0.19363(17)	0.45923(11)	0.0372(5)
C5	1.02702(19)	0.12856(16)	0.48157(11)	0.0353(5)
C6	0.96894(17)	0.14540(14)	0.53817(10)	0.0283(4)
C7	0.84901(15)	0.36735(12)	0.62830(9)	0.0208(4)
C8	0.84934(16)	0.43488(13)	0.67728(10)	0.0247(4)
C9	0.80292(18)	0.52107(14)	0.66417(11)	0.0308(5)
C10	0.75623(17)	0.54042(14)	0.60239(11)	0.0309(4)
C11	0.75859(19)	0.47489(15)	0.55253(11)	0.0345(5)
C12	0.80470(18)	0.38850(14)	0.56520(10)	0.0303(4)
C13	0.79651(15)	0.16938(13)	0.64292(9)	0.0224(4)
C14	0.82207(19)	0.08073(14)	0.66632(11)	0.0318(5)
C15	0.7437(2)	0.01159(16)	0.66370(12)	0.0414(6)

TABLE 4.7 continued.

C16	0.6392(2)	0.03060(18)	0.63872(12)	0.0449(6)
C17	0.61324(19)	0.11770(19)	0.61560(13)	0.0432(6)
C18	0.69184(17)	0.18772(15)	0.61720(11)	0.0305(4)
C19	0.4656(4)	0.3404(4)	0.7409(3)	0.0421(11)
Cl1	0.56085(6)	0.40487(6)	0.69085(4)	0.0589(2)
Cl2	0.47536(19)	0.23525(11)	0.73498(13)	0.0735(7)
P1	0.90662(4)	0.25377(3)	0.64648(3)	0.01831(11)
Pd1	1.0000	0.251176(12)	0.7500	0.01774(7)

TABLE 4.8 Bond lengths (Å) for $[PdBr_2(PPh_3)_2]$ mlm4.

Br2-Pd1	2.4287(12)	C1-C6	1.385(3)
C1-C2	1.395(3)	C1-P1	1.827(2)
C2-C3	1.381(3)	C2-H2	0.9500
C3-C4	1.381(4)	C3-H3	0.9500
C4-C5	1.377(3)	C4-H4	0.9500
C5-C6	1.395(3)	C5-H5	0.9500
C6-H6	0.9500	C7-C8	1.389(3)
C7-C12	1.394(3)	C7-P1	1.818(2)
C8-C9	1.390(3)	C8-H8	0.9500
C9-C10	1.376(3)	C9-H9	0.9500
C10-C11	1.384(3)	C10-H10	0.9500
C11-C12	1.389(3)	C11-H11	0.9500
C12-H12	0.9500	C13-C18	1.385(3)
C13-C14	1.396(3)	C13-P1	1.817(2)
C14-C15	1.384(3)	C14-H14	0.9500
C15-C16	1.380(4)	C15-H15	0.9500
C16-C17	1.375(4)	C16-H16	0.9500
C17-C18	1.396(3)	C17-H17	0.9500
C18-H18	0.9500	C19-C19#1	0.902(9)
C19-Cl2	1.529(6)	C19-Cl1#1	1.708(5)
C19-Cl2#1	1.742(5)	C19-Cl1	1.833(5)

TABLE 4.8 continued.

Cl1-C19#1	1.708(5)	Cl2-Cl2#1	0.835(4)
Cl2-C19#1	1.742(6)	P1-Pd1	2.3341(12)
Pd1-P1#2	2.3341(13)	Pd1-Br2#2	2.4287(12)

#1 -x+1,y,-z+3/2 #2 -x+2,y,-z+3/2

TABLE 4.9 Bond angles (°) for $[PdBr_2(PPh_3)_2]$ mlm4.

C6-C1-C2	118.1(2)	C6-C1-P1	122.53(16)
C2-C1-P1	119.38(16)	C3-C2-C1	120.9(2)
C3-C2-H2	119.5	C1-C2-H2	119.5
C4-C3-C2	120.6(2)	C4-C3-H3	119.7
C2-C3-H3	119.7	C5-C4-C3	119.2(2)
C5-C4-H4	120.4	C3-C4-H4	120.4
C4-C5-C6	120.4(2)	C4-C5-H5	119.8
C6-C5-H5	119.8	C1-C6-C5	120.8(2)
C1-C6-H6	119.6	C5-C6-H6	119.6
C8-C7-C12	118.94(18)	C8-C7-P1	120.21(15)
C12-C7-P1	120.86(15)	C7-C8-C9	120.47(19)
C7-C8-H8	119.8	C9-C8-H8	119.8
C10-C9-C8	120.23(19)	C10-C9-H9	119.9
C8-C9-H9	119.9	C9-C10-C11	119.87(19)
C9-C10-H10	120.1	C11-C10-H10	120.1
C10-C11-C12	120.3(2)	C10-C11-H11	119.9
C12-C11-H11	119.9	C11-C12-C7	120.15(19)
C11-C12-H12	119.9	C7-C12-H12	119.9
C18-C13-C14	119.41(19)	C18-C13-P1	123.88(16)
C14-C13-P1	116.70(16)	C15-C14-C13	120.4(2)

TABLE 4.9, continued.

C15-C14-H14	119.8	C13-C14-H14	119.8
C16-C15-C14	119.9(2)	C16-C15-H15	120.1
C14-C15-H15	120.1	C17-C16-C15	120.1(2)
C17-C16-H16	119.9	C15-C16-H16	119.9
C16-C17-C18	120.6(2)	C16-C17-H17	119.7
C18-C17-H17	119.7	C13-C18-C17	119.6(2)
C13-C18-H18	120.2	C17-C18-H18	120.2
C19#1-C19-Cl2	87.56(19)	C19#1-C19-Cl1#1	83.1(6)
Cl2-C19-Cl1#1	128.6(4)	C19#1-C19-Cl2#1	61.30(18)
Cl2-C19-Cl2#1	28.64(18)	Cl1#1-C19-Cl2#1	110.1(3)
C19#1-C19-Cl1	67.7(5)	Cl2-C19-Cl1	114.1(3)
Cl1#1-C19-Cl1	108.5(3)	Cl2#1-C19-Cl1	109.4(3)
C19#1-Cl1-C19	29.2(3)	Cl2#1-Cl2-C19	90.0(2)
Cl2#1-Cl2-C19#1	61.39(17)	C19-Cl2-C19#1	31.1(3)
C13-P1-C7	108.60(9)	C13-P1-C1	103.23(9)
C7-P1-C1	102.84(9)	C13-P1-Pd1	110.83(7)
C7-P1-Pd1	111.36(6)	C1-P1-Pd1	119.19(8)
P1#2-Pd1-P1	178.15(2)	P1#2-Pd1-Br2#2	92.16(4)
P1-Pd1-Br2#2	87.81(4)	P1#2-Pd1-Br2	87.81(4)
P1-Pd1-Br2	92.16(4)	Br2#2-Pd1-Br2	178.215(12)

TABLE 4.10 Torsion angles (°) for $[PdBr_2(PPh_3)_2]$ mlm4.

C6-C1-C2-C3	0.2(3)	P1-C1-C2-C3	179.84(19)
C1-C2-C3-C4	0.0(4)	C2-C3-C4-C5	0.2(4)
C3-C4-C5-C6	-0.6(4)	C2-C1-C6-C5	-0.6(3)
P1-C1-C6-C5	179.73(16)	C4-C5-C6-C1	0.9(3)
C12-C7-C8-C9	2.1(3)	P1-C7-C8-C9	-178.35(16)
C7-C8-C9-C10	-0.1(3)	C8-C9-C10-C11	-2.1(3)
C9-C10-C11-C12	2.1(3)	C10-C11-C12-C7	-0.1(3)
C8-C7-C12-C11	-2.1(3)	P1-C7-C12-C11	178.44(17)
C18-C13-C14-C15	0.2(3)	P1-C13-C14-C15	-178.22(17)
C13-C14-C15-C16	-1.0(4)	C14-C15-C16-C17	0.9(4)
C15-C16-C17-C18	-0.1(4)	C14-C13-C18-C17	0.6(3)
P1-C13-C18-C17	178.88(17)	C16-C17-C18-C13	-0.6(3)
Cl2-C19-Cl1-C19#1	-76.4(3)	Cl1#1-C19-Cl1-C19#1	74.1(5)
Cl2#1-C19-Cl1-C19#1	-46.0(3)	C19#1-C19-Cl2-Cl2#1	22.3(8)
Cl1#1-C19-Cl2-Cl2#1	-56.8(5)	Cl1-C19-Cl2-Cl2#1	86.5(5)
Cl1#1-C19-Cl2-C19#1	-79.2(7)	Cl2#1-C19-Cl2-C19#1	-22.3(8)
Cl1-C19-Cl2-C19#1	64.2(6)	C18-C13-P1-C7	12.1(2)
C14-C13-P1-C7	-169.60(15)	C18-C13-P1-C1	-96.61(18)
C14-C13-P1-C1	81.74(17)	C18-C13-P1-Pd1	134.68(16)
C14-C13-P1-Pd1	-46.98(17)	C8-C7-P1-C13	112.77(17)

TABLE 4.10 continued.

C12-C7-P1-C13	-67.74(18)	C8-C7-P1-C1	-138.31(16)
C12-C7-P1-C1	41.19(19)	C8-C7-P1-Pd1	-9.53(18)
C12-C7-P1-Pd1	169.96(15)	C6-C1-P1-C13	-17.04(19)
C2-C1-P1-C13	163.31(17)	C6-C1-P1-C7	-129.98(17)
C2-C1-P1-C7	50.38(19)	C6-C1-P1-Pd1	106.30(17)
C2-C1-P1-Pd1	-73.34(18)	C13-P1-Pd1-P1#2	-136.45(8)
C7-P1-Pd1-P1#2	-15.45(7)	C1-P1-Pd1-P1#2	104.01(7)
C13-P1-Pd1-Br2#2	-47.31(7)	C7-P1-Pd1-Br2#2	73.69(7)
C1-P1-Pd1-Br2#2	-166.85(7)	C13-P1-Pd1-Br2	134.47(7)
C7-P1-Pd1-Br2	-104.52(7)	C1-P1-Pd1-Br2	14.94(7)

Symmetry transformations used to generate equivalent atoms:

#1 -x+1,y,-z+3/2 #2 -x+2,y,-z+3/2

TABLE 4.11 Anisotropic atomic displacement parameters ($Å^2$) for $[PdBr_2(PPh_3)_2]$ mlm4**.**

The anisotropic atomic displacement factor exponent takes the form: $-2\pi^2 [h^2a^{*2} U_{11} + ... + 2hka^* b^* U_{12}]$

	U_{11}	U_{22}	U_{33}	U_{23}	U_{13}	U_{12}
Br2	0.02545(12)	0.02853(13)	0.02741(13)	-0.00056(7)	0.00366(9)	0.00220(7)
C10	0.215(9)	0.0233(8)	0.0188(9)	-0.0002(7)	-0.0006(7)	0.0007(7)
C2	0.0378(12)	0.0324(11)	0.0304(11)	-0.0044(9)	0.0082(9)	-0.0097(9)
C3	0.0383(13)	0.0485(13)	0.0356(13)	0.0018(11)	0.0117(10)	-0.0102(11)
C4	0.0347(11)	0.0512(14)	0.0261(11)	-0.0009(10)	0.0073(9)	0.0090(10)
C5	0.0438(13)	0.0334(11)	0.0289(11)	-0.0070(9)	0.0044(9)	0.0070(10)
C6	0.0337(11)	0.0244(10)	0.0271(10)	-0.0016(8)	0.0032(8)	0.0004(8)
C7	0.0226(9)	0.0174(8)	0.0225(9)	0.0016(7)	0.0014(7)	-0.0013(7)
C8	0.0287(10)	0.0224(9)	0.0229(9)	0.0012(7)	0.0009(8)	0.0000(7)
C9	0.0408(12)	0.0207(9)	0.0315(11)	-0.0013(8)	0.0074(9)	0.0033(8)
C10	0.0348(11)	0.0222(9)	0.0363(12)	0.0086(8)	0.0075(9)	0.0054(8)
C11	0.0440(13)	0.0307(11)	0.0283(11)	0.0073(9)	-0.0032(9)	0.0064(9)
C12	0.0416(12)	0.0242(10)	0.0248(10)	-0.0003(8)	-0.0032(9)	0.0035(9)
C13	0.0261(9)	0.0233(9)	0.0179(9)	-0.0031(7)	0.0034(7)	-0.0054(7)

TABLE 4.11 continued

C14	0.0411(12)	0.0239(10)	0.0302(11)	0.0030(8)	-0.0011(9)	-0.0072(9)
C15	0.0644(17)	0.0264(11)	0.0341(12)	-0.0028(9)	0.0091(11)	-0.0175(11)
C16	0.0519(15)	0.0446(14)	0.0395(13)	-0.0151(11)	0.0145(11)	-0.0311(12)
C17	0.0284(11)	0.0554(15)	0.0456(14)	-0.0129(12)	0.0021(10)	-0.0153(11)
C18	0.0273(10)	0.0325(11)	0.0317(11)	-0.0047(8)	0.0011(8)	-0.0036(8)
C19	0.028(2)	0.059(3)	0.039(3)	-0.006(2)	0.003(2)	-0.0039(19)
Cl1	0.0621(4)	0.0687(5)	0.0473(4)	0.0082(3)	0.0179(3)	0.0016(4)
Cl2	0.074(2)	0.0632(8)	0.086(2)	-0.0144(9)	0.0365(13)	-0.0214(9)
P1	0.0200(2)	0.0164(2)	0.0185(2)	-0.00062(16)	0.00012(18)	-0.00118(15)
Pd1	0.01964(11)	0.01574(11)	0.01777(11)	0.000	0.00009(8)	0.000

TABLE 4.12 Hydrogen atom coordinates and isotropic atomic displacement parameters ($Å^2$) for $[PdBr_2(PPh_3)_2]$ mlm4.

	x/a	y/b	z/c	U
H2	1.0636	0.3505	0.5717	0.040
H3	1.1608	0.3214	0.4780	0.049
H4	1.1388	0.1819	0.4209	0.045
H5	1.0170	0.0718	0.4583	0.042
H6	0.9205	0.0996	0.5534	0.034
H8	0.8815	0.4220	0.7200	0.030
H9	0.8034	0.5668	0.6980	0.037
H10	0.7224	0.5987	0.5940	0.037
H11	0.7286	0.4890	0.5095	0.041
H12	0.8060	0.3437	0.5308	0.036
H14	0.8937	0.0678	0.6841	0.038
H15	0.7619	-0.0488	0.6791	0.050
H16	0.5851	-0.0166	0.6375	0.054
H17	0.5412	0.1303	0.5984	0.052
H18	0.6736	0.2476	0.6008	0.037

4.5 – REFERENCES

1. (a) Boffa, L. S.; Novak, B. M. *Chem. Rev*. **2000**, *100*, 1479. (b) Ittel, S. D.; Johnson, L. K.; Brookhart, M. *Chem. Rev*. **2000**, *100*, 1169.
2. (a) Liu, S. H.; Elyashiv, S.; Sen, A. *J. Am. Chem. Soc.* **2001**, *123*, 12738-12739 (b) Elyashiv, S.; Greinert, N.; Sen, A. *Macromolecules* **2002**, *35*, 7521-7526. (c) Gu, B.; Liu, S.; Leber, D.; Sen, A. *Macromolecules* **2004,** *37*, 51425-5144 (d) Liu, S.; Sen, A. *J. Polym. Sci., Part A: Polym. Chem.* **2004**, *42*, 6175-6192. (e) Tian, G.; Boone, H. W.; Novak, B. M. *Macromolecules*, **2001**, *34*, 7656-7663. (f) Venkatesh, R.; Klumperman, B. *Macromolecules* 2004, *37*, 1226-1233. (g) Vankatesh, R.; Harrison, S.; Haddleton, D. M.; Klumperman, B. *Macromolecules* 2004, *37*, 4406-4416.
3. Nagel, M.; Poli, D.; Sen, A. *Macromolecules* **2005,** *38*, 7262-7265.
4. Brintzinger, H. H.; Fischer, D.; Mulhaupt, R.; Reiger, B.; Waymouth, R. M. *Angew. Chem,. Int. Ed. Engl.* **1995**, *34*, 1143-1170.
5. (a) Mecking, S.; Johnson, L. K.; Wang, L.; Brookhart, M. *J. Am. Chem. Soc.* **1998**, *120*, 888-899. (b) Drent, E.; Rudmer, D.; Ginkel, R.; Oort, B.; Pugh, R. *Chem. Commun.*, **2002**, 744-745.
6. (a) Stibrany, R. T.; Schulz, D. N.; Kacker, S.; Patil, A. O.; Baugh, L. S.; Rucker, S. P.; Zushma, S.; Berluche, E.; Sissano, J. A. *Macromolecules* **2003**, *36*, 8584-8586. (b) Younkin, T. R.; Connor, E. F.; Henderson, J. I.; Friedrich, S. K.; Grubbs, R. H.; Bansleben, D. A. *Science* **2000**, *287*, 460-462. (c) Nagel, M.;

Paxton, W. F.; Sen, A.; Zakharov, L.; Rheingold, A. L. *Macromolecules* **2004**, *37*, 9305-9307.

7. (a) Elia, C.; Elyashiv-Barad, S.; Sen, A.; Lopez-Fernandez, R.; Albeniz, A. C.; Espinet, P. *Organometallics*, **2002**, *21*, 4249-4256. (b) Albeniz, A. C.; Espinet, P.; Lopez-Fernandez, R. *Organometallics*, **2003**, *22*, 4206-4212. (c) Tian, G.; Boone, H. W.; Novak, B. M. *Macromolecules* **2001**, *34*, 7656-7663.

8. (a) Philipp, D. M.; Muller, R. P.; Goddard, W. A.; McAdon, M.; Mullin, M. *J. Am. Chem. Soc.* **2002**, *124*, 10198-10210. (b) Michalak, A.; Ziegler, T. *J. Am. Chem. Soc.* **2001**, *123*, 12266-12278.

9. (a) Mohring, V. M.; Fink, G. *Agnew. Chem., Int. Ed. Engl.* 1985, *24*, 1001-1003. (b) Shultz, L. H.; Tempel, D. J.; Brookhart, M. *J. Am. Chem. Soc.* 2001, *123*, 11539-11555. (c) Waltman, A. W.; Younkin, T. R.; Grubbs, R. H. *Organometallics*, 2004, *23*, 5121-5123.

10. Tolman, C. A. *Chem Rev.* 1977, *77*, 313-348.

11. Olmstead, M. M.; Pin-pin, W.; Ginwalla, A. S.; Balch, A. L. *Inorg. Chem.*, 2000, *39*, 4555-4559.

CHAPTER 5 – REARRANGEMENT AND DECOMPOSITION OF METAL-ALKYL SPECIES: RELEVANCE TO METAL-MEDIATED POLYMERIZATION OF POLAR VINYL MONOMERS

5.1 – INTRODUCTION

In the previous chapter, the instability of the palladium-alkyl bond with an ester group α to the metal center was clearly demonstrated. This instability and propensity to decompose both by β-hydrogen elimination and homolytic cleavage of the palladium-alkyl bond has plagued the development of successful metal catalysts for the insertion polymerization of acrylate monomers. To this point, only a very limited number of successful catalysts of this type have emerged.[1,2] One of these systems that copolymerize acrylates through an insertion mechanism is by Brookhart and involves cationic Pd(II)-based complexes of the general type, [(N^N)Pd(Me)(L)][B(Ar_f)$_4$] ((N^N) = 2,3-Bis(2,6-di-isopropylphenylimino) butane), Ar_f = 3,5-$(CF_3)_2C_6H_3$, L = Et_2O).[1] This system is able to incorporate up to 15 mol % acrylate in copolymerizations with ethene and 1-alkenes. A novel feature of this system is the rearrangement that follows acrylate insertion resulting in the removal of the ester functionality from the α position to the metal, eventually forming a six-membered chelate, **1** (FIGURE 5.1).[2] This unique feature of the system prompted us to examine the stability of the complex upon opening of the six-membered chelate by forming a neutral species.

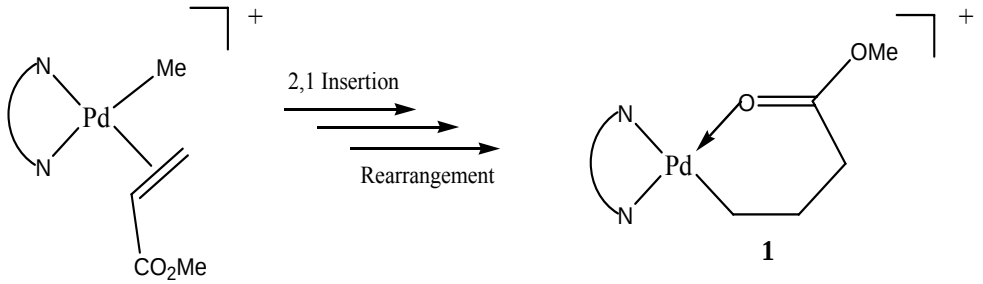

FIGURE 5.1 - "Chain-walking" rearrangement to form the stable 6-membered chelate.

5.2- RESULTS AND DISCUSSION

5.2.1 – DISRUPTION OF THE SIX-MEMBERED CHELATE

One equivalent of tetraphenylphosphonium bromide was added to complex 1 in CD_2Cl_2 to open the chelate ring and the reaction was monitored by ^{1}H-NMR spectroscopy. A complete and rapid conversion from **1** to **2** was observed (FIGURE 5.2). Compound **2** is not stable at room temperature and rearranges to **3** within minutes (66% overall yield). The driving force for this rearrangement is presumably the same as that for the 2,1-insertion of acrylates into Pd-C bonds; in the cationic Brookhart system the isomerization proceeds in the opposite direction because of the enhanced stability of the 6-membered chelate over the smaller chelate rings. Finally, **3** was found to decompose to yield methyl crotonate (68% overall yield) together with methyl butyrate (6% overall yield) and trace amounts of the diester, dimethyl suberate were also observed. While the transformations, **2** to **3** and **3** to methyl crotonate, can be explained by invoking the usual β-hydrogen abstraction/re-addition mechanism, the formation of methyl butyrate suggested the possibility that the methyl butyrate and at least some of the methyl crotonate arose through Pd-carbon bond homolysis in **3** followed by the well known disproportionation of the resultant radical. The fragmentation of the palladium-alkyl bond in **2** followed by radical-radical combination would lead to the formation of the diester. This was surprising because unlike **3**, bond homolysis in **2** leads to an unstabilized primary alkyl radical.

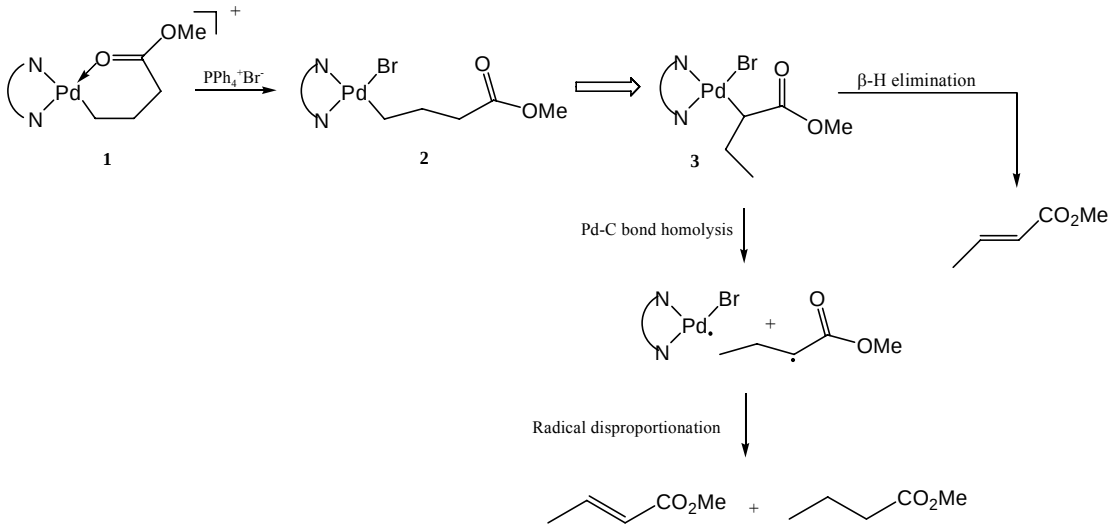

FIGURE 5.2 – Reaction pathway following disruption of the six-membered chelate.

Further support for the intermediate formation of radicals came from the observation that when the bromide salt was added to compound **1** in the presence of excess of methyl acrylate (MA) (0.0116 mol, 1.0 g) at room temperature, the homopolymerization of MA ensued (22% conversion, M_W = 60,760, and PDI = 1.71).

5.2.2 – PROBING FOR RADICAL FORMATION

To provide more convincing evidence for the presence of radicals, excess CBr_4 was added to **1** and $PPh_4^+Br^-$ (see TABLE 5.1). After several hours, the reaction mixture contained methyl 2-bromobutyrate (20% overall yield), the trapped product from homolytic cleavage of the palladium-alkyl bond in **3**. A second species, methyl 4-bromobuyrate, was also observed in a much greater concentration (38% overall yield).

There is a possibility that the observed alkyl bromides arise, not from radical trapping with CBr_4, but through reductive elimination from the corresponding Pd(alkyl)(Br) species, **2** and **3**. To further clarify the origin of the alkyl bromides, $NEt_4^+Cl^-$ was used to disrupt the chelate and CBr_4 was used as the radical trapping agent. In this case, alkyl radicals trapped by CBr_4 would generate bromides while reductive elimination would lead to the formation of chlorides. Only alkyl bromides were observed by GC and NMR spectroscopy, the yields being similar to those observed previously (TABLE 5.1). As a final control experiment, we verified that CBr_4 by itself did not react with **1**. Our observations clearly suggest that the palladium-alkyl species present in the system readily undergo bond homolysis to generate alkyl radicals.

Entry	Halide Salt	CBr_4 (mmol)	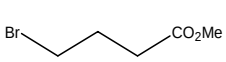	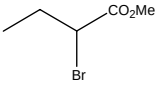	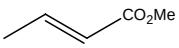	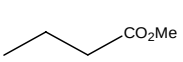
1	$Ph_4P^+Br^-$	0	---	---	68%	5.3%
2	$Ph_4P^+Br^-$	0.075	38%	20%	22%	5.6%
3	$Et_4N^+Cl^-$	0.075	33%	14%	22%	8.5%

TABLE 5.1 – Quantification of Products when CBr_4 is Present[a]

[a]Reaction conditions: 0.0136 mmol of **1**, 0.075 mmol of CBr_4,0.032 mmol of halide salt, 1 mL of CH_2Cl_2 [b] Without CBr_4.

5.2.3 – REACTION KINETICS AND THERMODYNAMICS

It is clear that there is rearrangement from **2** to **3**, and the formation of radicals resulting from the homolytic of both compounds **2** and **3.** This led us to examine the reaction kinetics and thermodynamics of this rearrangement and subsequent decomposition to uncover the mechanism of each. Both the conversion from **2** to **3** and the appearance of methyl crotonate yield a linear first order kinetic plots (FIGURES 5.3 AND 5.4). An Eyring analysis for the conversion of **2** to **3** over the temperature range of 5 to 29 °C gives $\Delta H^{\ddagger} = 15.6 \pm 1.1$ kcal/mol and $\Delta S^{\ddagger} = -12.9 \pm 5.7$ eu (FIGURE 5.5). The slightly negative value for $\Delta S^{\ddagger}$ suggests that this transition occurs through the ordered planar transition state synonymous with "chain-walking". Additionally, the thermodynamic data closely corresponds to the values obtained for the initial insertion of MA into the Pd-methyl bond (TABLE 5.2).

It may seem unlikely for complexes **2** or **3** to undergo β-H elimination because both lack the vacant coordination site needed for such a transition. However, by ^{1}H NMR we do observe the appearance of resonances corresponding to the free diimine ligand during the onset of these transitions. Rather than the formation of an unlikely 5 coordinate palladium center, we believe that one side of this bidentate ligand is freed to allow for this process to occur. Likewise, the dissociation of the bromide leading to ion pair formation does not appear to occur since the rate of the rearrangement did not decrease on moving from methylene chloride to less polar chlorobenzene (CH_2Cl_2: k, 0.039 sec^{-1}; PhCl: k, 0.093 sec^{-1}).

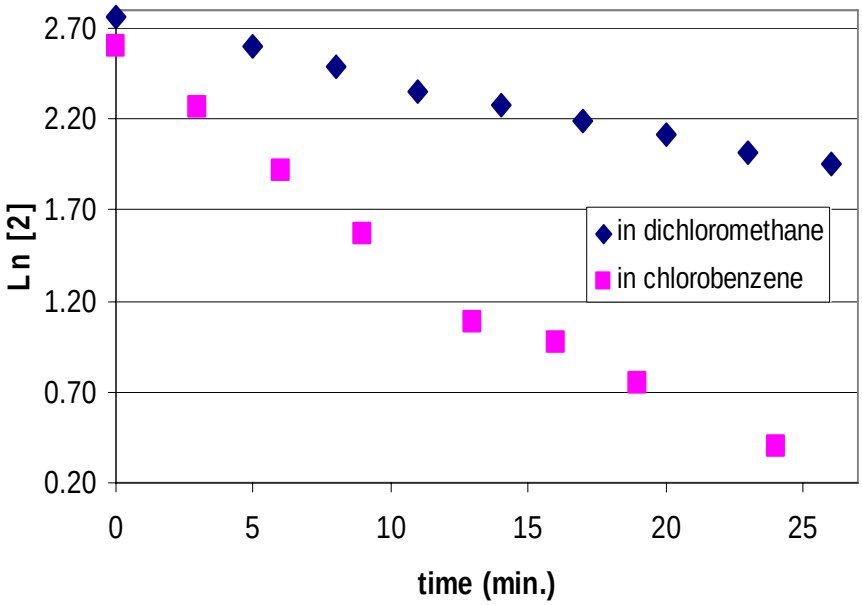

FIGURE 5.3– First order kinetic plot for the disappearance of **2.**

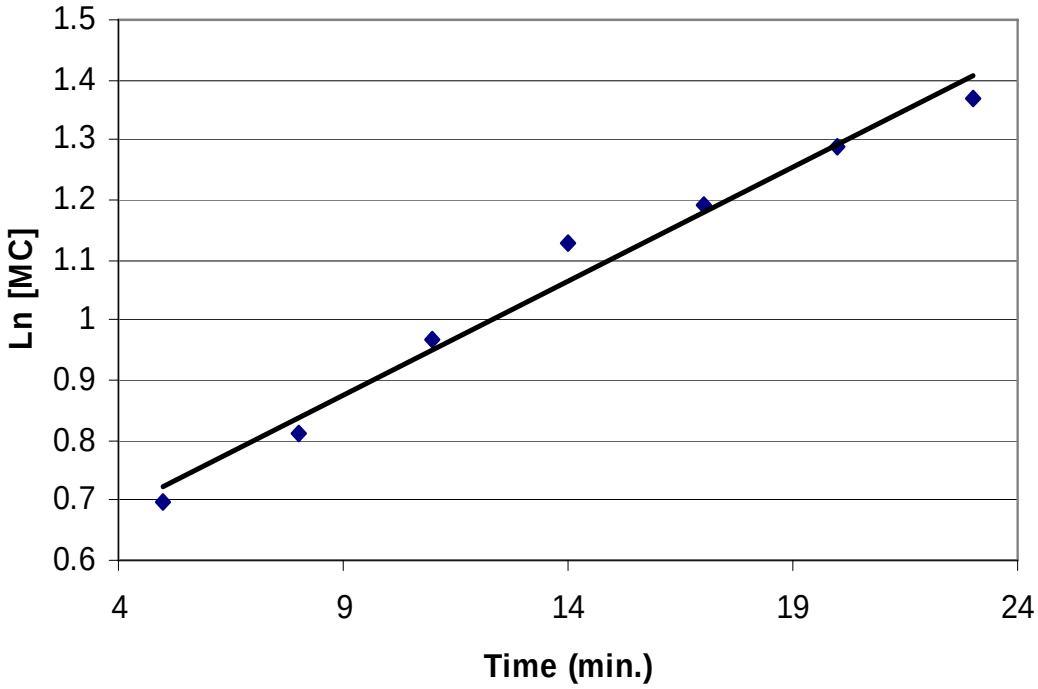

FIGURE 5.4 – First order kinetic plot for the appearance of methyl crotonate.

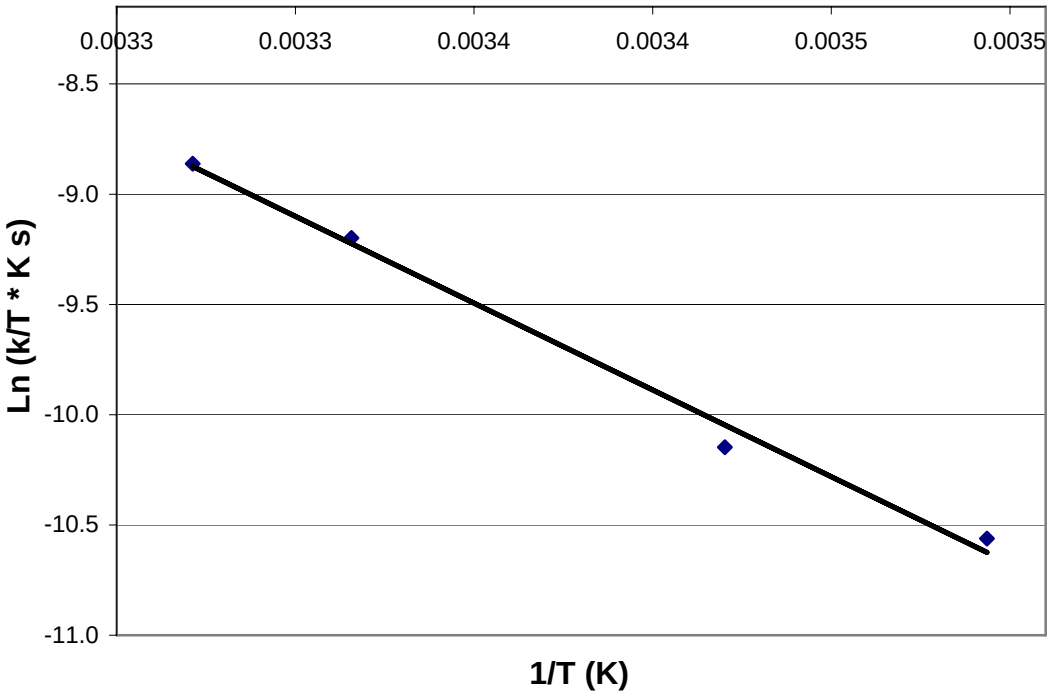

FIGURE 5.5 – Eyring plot for the conversion from **2** to **3.**

TABLE 5.2 – Comparison of Thermodynamic Data

	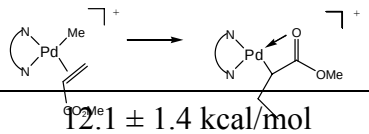	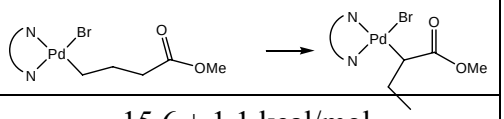
$\Delta H^{\ddagger}$	12.1 ± 1.4 kcal/mol	15.6 ± 1.1 kcal/mol
$\Delta S^{\ddagger}$	-14.1 ± 7.0 eu	-12.9 ± 5.7 eu
$\Delta G^{\ddagger}$	16.3 kcal/mol	19.5 kcal/mol

If in fact, this rearrangement is occurring through a β-hydrogen step, then the addition of excess ligand to the reaction mixture would have an effect on the rates of the transition. It is expected that additional ligand would compete for the vacant site needed for β-hydride elimination, and the reaction rate would decrease. However, in the presence of a five-fold excess of ligand, there is no change in rate for the transition from **2** to **3** (0.032 versus 0.038 sec^{-1} at 25 °C). This was surprising, but we discovered that in the presence of a five-fold excessof ligand, the rate of the initial insertion and rearrangement of MA, known to occur by β-hydrogen elimination / readdition, is also unaffected. Finally, the decomposition of **3** to methyl crotonate, a known β-hydrogen elimination product, is halted in the presence of excess ligand. This suggests that the "chain-walking" occurs in a concerted manner that is unaffected by additional ligand present, whereas the decomposition step is engaged in this competition.

These results are consistent with the scheme displayed in FIGURE 5.6. Upon disruption of the six-membered chelate, the palladium alkyl complex may either homolytically cleave or undergo β-hydrogen elimination / readdition, resulting in a complex analogous to the initial 2,1 methyl acrylate insertion product. Based on the quantification of products both with and without the radical trapping agent, CBr_4, present, it is clear that "chain-walking" is preferred 3 to 1 over homolytic cleavage of complex **2**.

Following the decomposition of **3,** there is a relatively small amount of methyl 2-bromobutyrate formed in the presence of CBr_4 and a much higher amount of methyl crotonate compared to methyl butyrate. The latter suggests that the predominant route to methyl crotonate is by traditional β-hydrogen abstraction from **3** rather than Pd-C bond

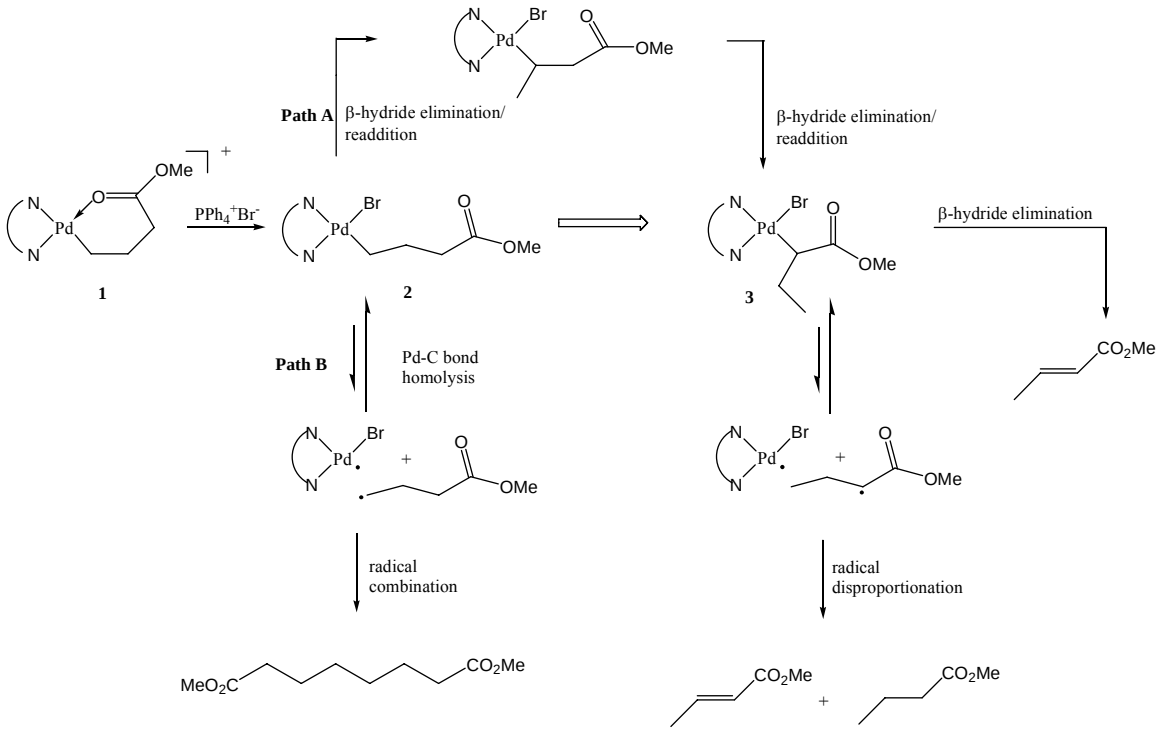

FIGURE 5.6 – Rearrangement and decomposition pathways upon disruption of the six-

homolysis. Consistent with this was the observation that the addition of excess ligand, the subsequent decomposition of **3** was halted.

5.3 CONCLUSIONS

Our findings illustrate the propensity of Pd-alkyl species to undergo Pd-C bond homolysis. While in the present instance homolytic decomposition of **2** is more facile than **3**, the Pd-C bond homolysis of alkyl groups with ester functionality α to the metal has been documented elsewhere.[5a,b] Thus, simply preventing the coordination of the functionality present on the polar vinyl monomer will not necessarily result in a viable system for insertion polymerization. Indeed, it appears that the success of the Brookhart system in copolymerizing acrylates is due to stable chelate formation following acrylate insertion (complex **1**) but, the price paid for chelate formation is slow polymerization and the placement of the functionality predominantly at the branch ends.

Our results illustrate the reversibility of "chain-walking", and again reiterate the high propensity for radical formation following the insertion of methyl acrylate into the palladium-alkyl bond. In the future, this should be taken into consideration when designing a catalyst for the insertion polymerization of acrylates.

5.4 EXPERIMENTAL PROCEDURES

5.4.1 – GENERAL CONSIDERATIONS

All manipulations involving air/moisture sensitive compounds were carried out either in a dry N_2 glovebox, or under N_2, using Schlenk techniques. Pentachloroethane was used as an internal standard for both ^{1}H-NMR kinetic experiments and quanitative analysis using GC. 1-D ^{1}H-NMR spectra were recorded on a Bruker DPX-300 (300 MHz) or Bruker AMX-360 (360 MHz) spectrometer. 2-D COSY spectra were recorded on a Bruker DMX-400 (400 MHz) spectrometer (FIGURE 5.7). ^{1}H NMR chemical shifts are reported in parts per million (ppm) relative to residual protiated solvent (CD_2Cl_2, 5.32 ppm). Quantification of methyl butyrate and methyl crotonate was done using gas chromatography on an Agilent 5890 Series II GC using a RTX-5 split capillary column (Restek) connected to an FID detector. With an injector temperature of 250°C, the sample was heated from 60° to 150°C at a ramp rate of 5 °C/minute.

5.4.2 – MATERIALS

[$PdBr_2(PPh_3)_2$]Dichloromethane was distilled, degassed and stored over molecular sieves. Methyl acrylate (MA, 99%) was vacuum distilled from CaH_2 and stored under N_2. Methylene chloride–d_2 was received from Cambridge Isotope Laboratories and used directly from one gram ampoules. The diimine ligand, 2,3-Bis(2,6-di-*i*-propylphenylimine)butane

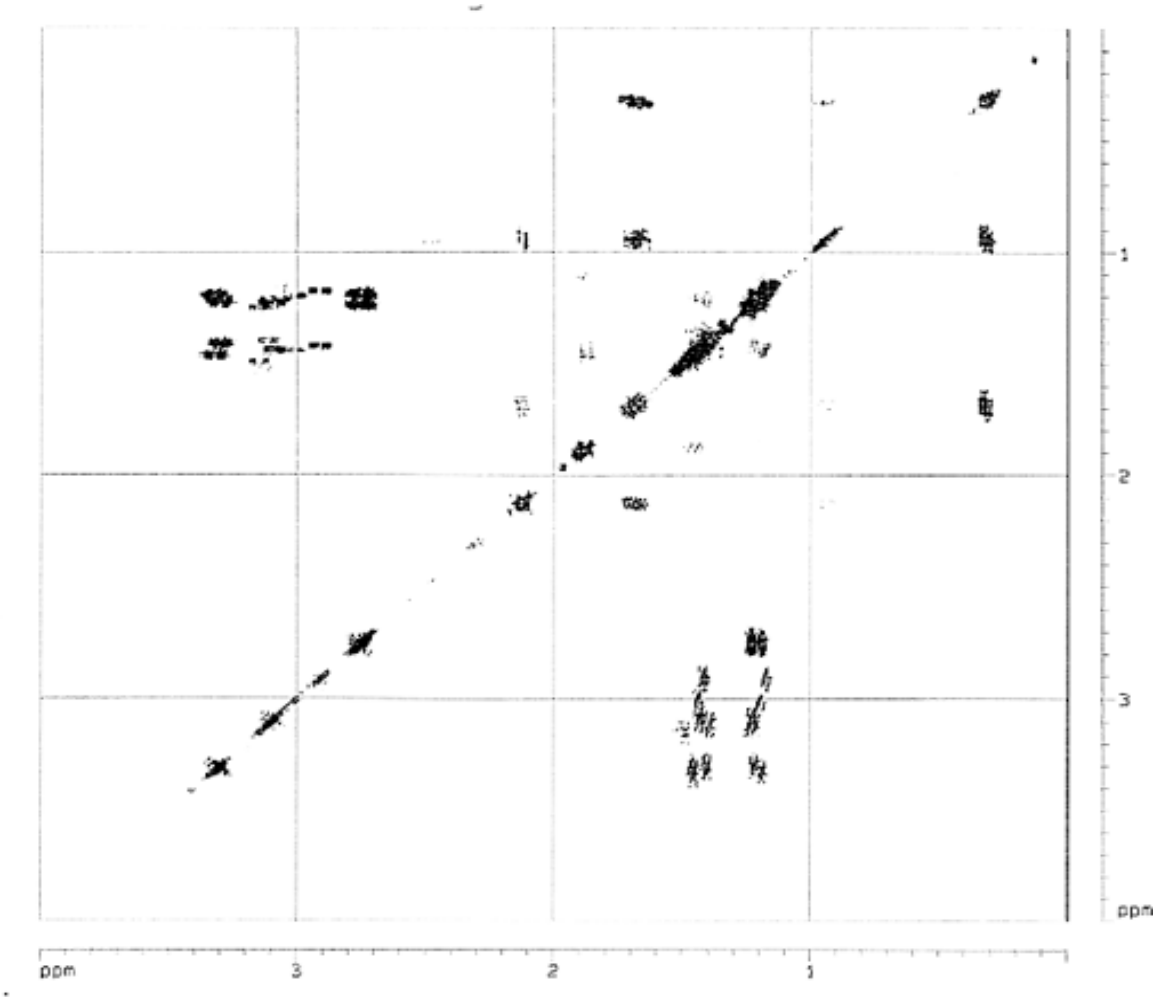

FIGURE 5.7 - COSY NMR Spectrum of **3** (CD_2Cl_2) (400 MHz).

(98%) and tetraphenylphosphonium bromide (PPh_4Br) were purchased from Strem and Alrich respectively, and used as received.

5.4.3 – SYNTHESIS OF [ArN=C(Me)=NAr)Pd($(CH_3)_2CO_2CH_3$)(Br) (Ar = 2,6-C_6H_3(*i*-Pr)$_2$ (2).

Compound **1** was prepared according to the literature.[1] A solution containing **1** (20 mg, 0.014 mmol) in CD_2Cl_2 (2 g, 23 mmol) was prepared. To this solution, 1 equivalent of PPh_4Br (13.7 mg, 0.033 mmol) was added. The mixture was stirred at room temperature and quickly turned a deeper orange. According to ^{1}H NMR spectrum, **1** completely reacts with the PPh_4Br after 5 minutes, to give compound **2.** **2:** ^{1}H NMR (CD_2Cl_2, 300 MHz, ppm) 7.72 and 7.59 (s, 3H each, $C_6H_3Me_2$ and C'$_6H_3Me_2$), 3.49 (s, 3H, O*Me*), 3.15 (septet, 2H, J = 6.78, C*H*Me_2), 2.96 (septet, 2H, J = 6.80, C'*H*Me_2), 2.09 and 2.04 (s, 3H each, N=C(*Me*)-C'(*Me*)=N), 1.9 (t, J = 6.1, 2H, CH_2C(O)), 1.43 (t, 2H, J = 5.69 PdCH_2), 1.42, 1.34, 1.29, and 1.23 (d, 3H each, J = 6.82 – 7.07, CH*MeMe'*, C'H*MeMe'*), 1.35 (m, 2H, PdCH$_2$CH_2CH$_2$C(O)).

5.4.4 – SYNTHESIS OF [ArN=C(Me)=NAr)Pd(CHEtCO_2CH_3)(Br) (Ar = 2,6-C_6H_3(*i*-Pr)$_2$ (3).

After stirring at room temperature for longer than 10 minutes, the conversion from **2** to **3** can be observed. **3:** ^{1}H NMR (CD_2Cl_2, 300 MHz, ppm) and COSY NMR (CD_2Cl_2, 400 MHz, ppm) 7.72 and 7.59 (s, 3H each, $C_6H_3Me_2$ and C'$_6H_3Me_2$), 3.40 (s,

3H, O*Me*), 3.15 (septet, 2H, J = 6.78, C*H*Me_2), 2.96 (septet, 2H, J = 6.80, C'*H*Me_2), 2.10 (t, J = 6.1, 2H, PdCHCHH'CH_3), 2.09 and 2.04 (s, 3H each, N=C(*Me*)-C'(*Me*)=N), 1.42, 1.34, 1.29, and 1.23 (d, 3H each, J = 6.81 – 7.07, CH*MeMe'*), 1.65 and 0.95 (m, 1H each, PdCHC*HH'*CH_3), 0.30 (t, 2H, J = 5.69, PdC*H*).

5.4.5 – REACTION KINETICS

On the bench top, a solution containing **1** (20 mg, 0.014 mmol) in CD_2Cl_2 (2 g, 23 mmol) was prepared. Separately, PPh_4Br (13.7 mg, 0.033 mmol) and one drop of pentachloroethane (PCE) were added to a shorty vial. To this vial, the first solution was added, quickly shaken and added to an NMR tube, and a ^1H NMR was taken within five minutes. A proton NMR was then taken approximately every three minutes for at least 25 minutes. The disappearance of complex **2** was calculated by integration of the standard PCE peak at 6.25 ppm versus the peak from the methoxy corresponding to complex **2** at 3.49 ppm. This reaction was repeated for a number of temperatures (10, 16, 23, 25, and 29° C). When the kinetics for the rearrangement were repeated in chlorobenzene, the same reaction procedure was used, but the halide salt, tetrabutylammoniumchloride (Bu_4NCl) was used in place of PPh_4Br for solubility reasons.

From the same ^1H NMR's obtained from the above experiments, the rate of appearance of methyl crotonate was also calculated. This was done again using the standard PCE peak and the integration of the corresponding methoxy peak of methyl crotonate at 3.7 ppm. The mmoles produced were calculated from a standard plot

generated from ^{1}H NMR's of varying amounts of PCE and methyl crotonate. From this information, a first order kinetic plot was made.

5.4.6 – REARRANGEMENT IN THE PRESENCE OF EXCESS LIGAND

A solution containing **1** (20 mg, 0.014 mmol) in CD_2Cl_2 (2 g, 23 mmol) was prepared. To this solution, an excess the same N^N ligand that is in complex **1** (66 mg, 0.16 mmol) was added. After the excess ligand was completely dissolved PPh_4Br (13.7 mg, 0.033 mmol) was added to the solution. The kinetics were studied by ^{1}H NMR as described in section 5.4.5.

5.4.7 – RADICAL TRAPPING EXPERIMENTS

In an N_2 filled glove box, a solution containing **1** (20 mg, 0.014 mmol) in CH_2Cl_2 (2 g, 23 mmol) was prepared. To this solution, an excess of CBr_4 (25mg, 0.075mmol) was added. After the CBr_4 was completely dissolved, the halide salt, PPh_4Br or Et_4NCl, (0.033 mmol) was added to the solution. This solution was allowed to react for several hours at room temperature. One drop of PCE was added to the reaction just before gas chromatography was used to identify and quantify the decomposition products that were present. The mmoles of each decomposition product were determined from standard plots for each compound. These standard plots were made by making five standard solutions of the decomposition products (methyl butyrate, methyl crotonate, methyl 2-

bromobutyrate, methyl 4-bromobutyrate, and methyl suberate), and varying the amount of each compound versus the amount of PCE present.

5.5 – REFERENCES

1. Mecking, S.; Johnson, L. K.; Wang, L.; Brookhart, M. *J. Am. Chem. Soc.* **1998**, *120*, 888-899.

2. Drent, E.; Rudmer, D.; Ginkel, R.; Oort, B.; Pugh, R. *Chem. Commun*., **2002**, 744-745.

VITA

Megan Nagel was born on February 13, 1980 in Jeannette, Pennsylvania. After graduating from Hempfield High School, she attended Slippery Rock University in Slippery Rock, Pennsylvania. While at Slippery Rock, she performed research under the guidance of Dr. Paul Birckbichler, studying an animal model for type II diabetes. She also spent the summer of 2001 at Penn State University working on the release mechanism of neurotransmitters under Dr. Andrew Ewing. After receiving her B.S. in chemistry from Slippery Rock University in the Spring of 2002, she moved to State College, Pennsylvania and began her research under the guidance of Dr. Ayusman Sen. While she was at Penn State, she was the recipient of the Braddock Graduate Fellowship, the Roberts Graduate Fellowship, and the Dalalian Graduate Fellowship. She received her Ph.D. in the Summer of 2006. After graduation, Megan moved to St. Paul, Minnesota to be an assistant professor of chemistry at Bethel University.